

1 **Observing ocean ecosystem responses to volcanic ash**

2 K. M. Bisson<sup>1\*</sup>, S. Gassó<sup>2,3</sup>, N. Mahowald<sup>4</sup>, S. Wagner<sup>5</sup>, B. Koffman<sup>6</sup>, S.A. Carn<sup>7</sup>, S. Deutsch<sup>4</sup>,  
3 E. Gazel<sup>4</sup>, S. Kramer<sup>8</sup>, N. Krotkov<sup>3</sup>, C. Mitchell<sup>9</sup>, M. E. Pritchard<sup>4</sup>, K. Stamieszkin<sup>9</sup>, and C.  
4 Wilson<sup>10</sup>

5  
6 <sup>1</sup> Department of Botany and Plant Pathology, Oregon State University, Corvallis, Oregon, USA

7 <sup>2</sup> Earth System Science Interdisciplinary Center, University of Maryland, College Park,  
8 Maryland, USA

9 <sup>3</sup> NASA Goddard Space Flight Center, Greenbelt, Maryland, USA

10 <sup>4</sup> Earth and Atmospheric Sciences, Cornell University, Ithaca, New York, USA

11 <sup>5</sup> Earth and Environmental Sciences, Rensselaer Polytechnic Institute, Troy, New York, USA

12 <sup>6</sup> Department of Geology, Colby College, Waterville, Maine, USA

13 <sup>7</sup> Department of Geological and Mining Engineering and Sciences, Michigan Technological  
14 University, Houghton, Michigan, USA

15 <sup>8</sup> Monterey Bay Aquarium Research Institute, Moss Landing, California, USA

16 <sup>9</sup> Bigelow Laboratory for Ocean Sciences, East Boothbay, Maine, USA

17 <sup>10</sup> NOAA Southwest Fisheries Center, Monterey, California, USA

18

19 \* corresponding author, bissonk@oregonstate.edu

20

21

22

23

24

25 **Abstract:** Volcanic eruptions can be catastrophic events, particularly when they occur in  
26 inhabited coastal environments. They also play important roles in climate and biogeochemical  
27 cycles, including through nutrient deposition in the ocean. Volcanic ash studies in the ocean have  
28 focused on the phytoplankton response, generally quantifying changes in chlorophyll-a  
29 concentration. Many gaps remain in addressing fundamental questions regarding why volcanic  
30 ash deposition may enhance or limit both phytoplankton growth and/or drive community  
31 composition shifts. Here we outline a wide, multidisciplinary vision for monitoring volcanic  
32 eruptions near ocean ecosystems from satellites, including considerations for characteristics of  
33 airborne volcanic ash and ash geochemistry in seawater. Ultimately, observations beyond  
34 chlorophyll-a are needed to quantify phytoplankton communities (including harmful algal  
35 blooms) and possible impacts across higher trophic levels. We synthesize relevant research from  
36 volcanic studies as well as atmospheric and ocean sciences to identify the ‘known unknowns’ in  
37 ash-ecosystem studies. Our goal is to move toward an improved understanding of how real-time  
38 and near-real-time monitoring of volcanic eruptions can help address societally relevant  
39 questions.

40

41 **Keywords:** volcano, phytoplankton, eruption, ecosystem

42 **Highlights:**

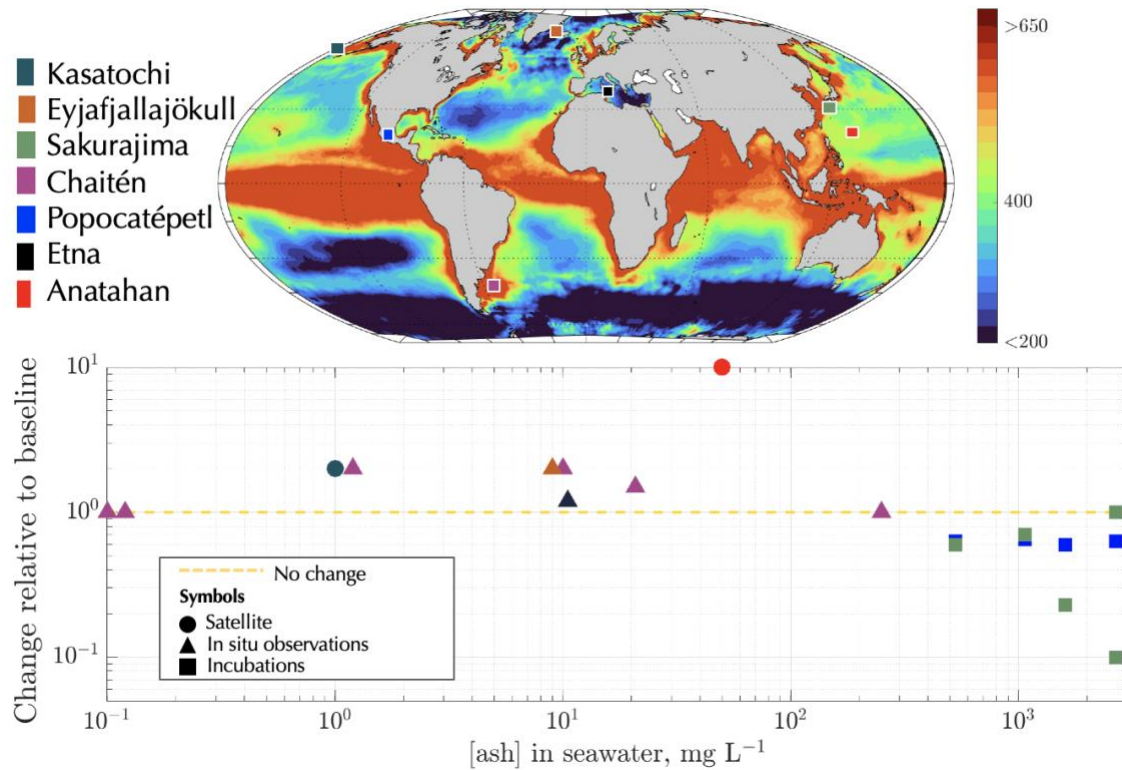
- 43 ● Volcanic eruptions elicit various optical responses and challenges for satellites
- 44 ● Ecosystem responses are nuanced and poorly understood
- 45 ● Improved understanding requires coupled atmosphere/ocean studies

46

47

48        **1. Introduction**

49            Volcanic eruptions are extreme events that have had measurable effects on terrestrial and  
50 marine ecosystem function throughout Earth’s history (Lee et al., 2018, Schmidt et al., 2012).  
51 Modern ocean ecosystem responses are relatively less studied than terrestrial responses, due in  
52 part to the challenges of observing volcanic ash (VA) impacts in situ, and because volcanic  
53 eruptions are commonly disastrous for society, while their impacts on ocean ecosystems are of  
54 secondary importance (Tayag and Punongbayan, 1994). The oceanographic community has only  
55 recently – in the last ~15 years – begun to consider whether it is possible to see a biological  
56 response to VA deposition using satellites and remote platforms. The focus on coupled volcanic-  
57 oceanic events in the literature largely centers on the principal volcanic eruptions that have  
58 elicited a profound ocean response through enhanced chlorophyll-a, leading to a general  
59 paradigm that volcanic eruptions fertilize the ocean by providing limiting nutrients (e.g., iron or  
60 manganese; Hamme et al., 2010, Browning et al, 2014, Wilson et al., 2019, Westberry et al.,  
61 2019, Barone et al., 2022). Substantial gaps remain in quantifying the full spectrum of  
62 phytoplankton responses to volcanic events, from low to high ash deposition rates across a range  
63 of chemical compositions (Figure 1). Can volcanic eruptions always be expected to fertilize the  
64 ocean, or are there situations in which ash in seawater will have no measurable impact, or even a  
65 negative effect on marine biota? Answering this question is not only scientifically interesting, but  
66 it has societal importance as coastal communities grapple with volcanic disasters and their  
67 repercussions on water quality, fisheries, and human health.



68

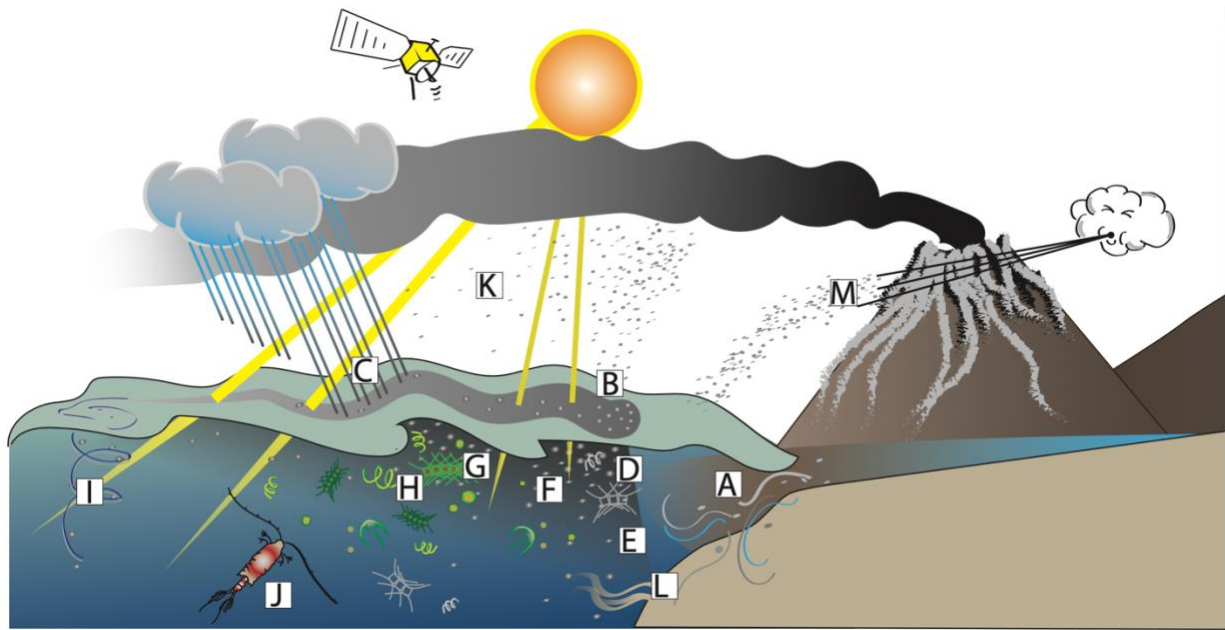
69 Figure 1. (top) Climatological average of net primary production,  $\text{mg C m}^{-2} \text{d}^{-1}$  from the carbon  
 70 based productivity model (Westberry et al. 2008). Locations with volcanic data are in colored  
 71 boxes. Note that satellite, in situ, and incubation results are all presented as colored squares.  
 72 (bottom) The relative change in chlorophyll-a concentration (circle and triangle symbols) and  
 73 growth rate (square symbols) relative to a baseline (i.e., value after ash addition divided by value  
 74 prior to ash addition) due to different concentrations of ash in seawater. Satellite values are taken  
 75 from Lin et al., 2011. In situ observations are from Mélançon et al., 2014, Browning et al., 2014  
 76 (and refs therein), and Achterberg et al., 2013. Incubations (with 2 different phytoplankton  
 77 compositions) are from Hoffmann et al., 2012.

78

79

The likelihood of an ocean biological response from phytoplankton (unicellular  
 80 photosynthetic protists that provide roughly half of the world's net primary production) to ash  
 81 deposition is a function of several factors (Figure 2). From the volcanic perspective, the main  
 82 factors are the VA composition and emission rate across the size spectrum of ash (Zimanowski et  
 83 al., 2003). From an atmospheric perspective, the properties of the VA (particle size, shape and  
 84 composition) change as VA is transported from its volcanic source to ocean regions (Langmann  
 85 et al., 2010). Ash may be dry-deposited (free fall of particles directly from the atmosphere) or

86 wet-deposited (deposition of material mixed with suspended water, e.g., rain, snow, ice, fog in  
87 the atmosphere) depending on the presence and phase of water in the atmosphere (Duggen et al.,  
88 2010; e.g., Delmelle et al., 2001, Kawaratani and Fujita, 1990). Ash first deposited on land can  
89 then be remobilized by winds or runoff, leading to delayed deposition in the ocean (Figure 2).  
90 Once in the ocean, ash viscosity (density) and geochemistry will affect its behavior in  
91 seawater, including its buoyancy, sinking, and solubility (Ayris and Delmelle, 2012). In the  
92 ocean, the degree to which phytoplankton are nutrient limited will affect any phytoplankton  
93 growth response to ash deposition (Hecky and Kilham, 1988), and different groups of  
94 phytoplankton respond differently to atmospheric deposition (Mahowald et al., 2017). The  
95 residence time and dilution of ash in water will be controlled by physical conditions and water  
96 mass circulation, in addition to mixing and resuspension events within the water column.  
97 Depending on ash deposition rate, ash layers in the surface ocean may limit light transmission to  
98 waters below, and ash may dilute phytoplankton as a food source in the water column,  
99 potentially decreasing encounter rates of phytoplankton and zooplankton (their predators).  
100 Ultimately, some or none of these characteristics may be available from remote platforms for any  
101 given volcanic eruption, due to the optically dense plumes obstructing various signals. Yet, given  
102 the episodic nature of volcanic eruptions, satellite remote sensing offers the only way to assess  
103 volcanic activities in real time (and synoptically) without physically traveling to the location by  
104 plane or ship. The availability of real-time (or near-real-time) observations are important for  
105 monitoring events to improve understanding of the role volcanoes play in influencing ocean  
106 ecosystems, and also may help provide aid to coastal communities experiencing disaster.



107

108 Figure 2. Conceptual illustration of coastal volcanic eruptions. A. Fluvial input of aged ash and  
 109 chromophoric dissolved organic matter (CDOM). B. Dry deposition. C. Wet deposition. D. Ash  
 110 leaching (potential toxicity given by grey phytoplankton). E. Shading due to ash microlayer. F.  
 111 Organic ligands enhance nutrient leaching. G. Enriched CDOM from increased particulate ash  
 112 concentration. H. Increased phytoplankton growth and biomass, community changes. I. Vertical  
 113 mixing enhances ash flux to depth. J. Possible trophic effects (direct or indirect). K. Higher light  
 114 attenuation in the atmosphere closer to the volcanic source compared to further away. L.  
 115 Resuspended ash and sediment from continental shelf. M. Remobilized ash.

116

117

In this review, we introduce a flexible multidisciplinary framework with which to

118

approach future remote sensing studies of volcanic ash in the ocean. We identify primary axes of

119

importance, namely, ‘Airborne volcanic ash characteristics,’ ‘Ash geochemistry in seawater,’

120

and ‘Ash impacts on ocean biota.’ In order to move toward a predictive understanding of ash

121

effects on ocean biology and biogeochemistry, these axes ideally will be considered in concert.

122

We argue that a multidisciplinary approach is needed, as quantifying ash concentration,

123

describing ash composition and behavior in seawater, and defining pre-existing ocean ecosystem

124

structure are critical and non-trivial components for anticipating ocean impacts. Here, we

125

identify the ‘known unknowns,’ or those parameters that are not able to be sensed from space but

126

are important to consider (including possible downstream effects on zooplankton and fish). We

127 discuss current progress from the viewpoint of lab-controlled studies and existing observations in  
128 situ, as well as uncertainties associated with attributing a remote sensing signal to a biological  
129 response to ash in the ocean. The framework presented here aims to move the field toward a  
130 diagnostic understanding of how satellite observations can help monitor real-time airborne and  
131 marine changes following volcanic eruptions.

## 132 **2. Airborne volcanic ash characteristics**

133 Volcanic ash (VA) is a broad term referring to the multiphase solid particulate matter  
134 emitted into the atmosphere by volcanic activity. VA physiochemical characteristics are critical  
135 to its impact on the Earth system because the composition and size of the ash will determine its  
136 interactions within the atmosphere. The chemical and mineralogical composition and particle  
137 size distribution of VA is complex and may consist of: juvenile, angular volcanic glass shards;  
138 crystal fragments derived from multiple mineral phases (e.g., quartz, feldspar, micas, pyroxenes,  
139 amphiboles, olivine); and lithic fragments eroded from the volcanic conduit and vent during  
140 eruption (Vogel et al., 2017, Heiken, 1974). In volcanic plumes, VA always coexists with  
141 volcanic gases (water vapor, CO<sub>2</sub>, SO<sub>2</sub>, halogens) and liquid or solid hydrometeors (i.e.,  
142 consisting of liquid or solid water particles) that can influence VA composition, element mobility  
143 and lifetime. Ionic and halide salts can also be incorporated into VA as the volcanic plume  
144 rapidly cools, and these salts may enhance the reactivity of VA above the plume (Ayris and  
145 Delmelle, 2012). VA will sink at different speeds depending on its size and density, and the  
146 soluble salt fraction is expected to quickly dissolve once the ash is deposited in seawater. The  
147 optical properties of the ash determine its interactions with incoming solar radiation and  
148 outgoing long wave radiation, as well as its interactions with clouds (Langmann, 2014).

149 In general, modeling top-of-atmosphere radiances while accounting for ash is challenging  
150 because VA has unknown composition and unknown refractive index, with unknown size and  
151 shape distributions (Krotkov et al. 1999a). Discriminating volcanic ash (VA) from metrological  
152 clouds (water and ice) and other aerosols (smoke, dust) requires advanced retrieval approaches,  
153 e.g., multiangle (MISR), polarization (POLDER, HARP), and spectral extension methods (UV  
154 Aerosol Index from TOMS, OMI/OMPS/GOME/TROPOMI). Aerosol layer height can be  
155 retrieved using O<sub>2</sub> absorption and/or multi-angle stereo techniques. From the inversion point of  
156 view, retrieval biases present a major challenge, because there are no good a-priori constraints on  
157 the inversion. Wrong a-priori (size, shape, refractive index) results in biased ash optical thickness  
158 and mass retrievals. Given all these challenges, there has been reasonable agreement between  
159 independent ultraviolet (UV) and infrared (IR) ash mass retrievals, as in the case of the Mt. Spurr  
160 eruption (Krotkov et al. 1999b). In addition, more comprehensive measurements of the complex  
161 refractive index of VA are becoming available (e.g., Deguine et al. 2023; Piontek et al. 2021;  
162 Reed et al. 2018), which will assist future VA ash mass retrievals.

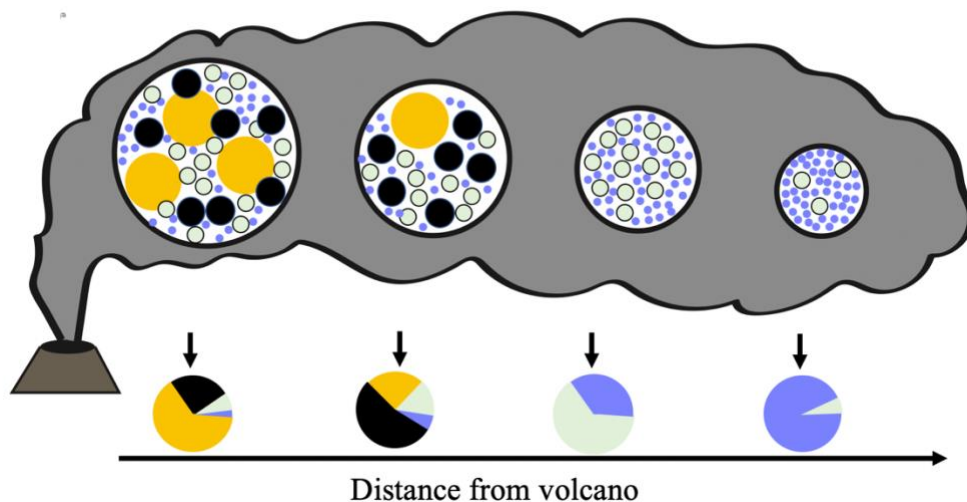
163 The chemical composition of VA is unknown prior to an eruption, and while it can often  
164 be constrained based on the prior eruptive history and tectonic setting of a volcano (Rogers,  
165 2015), this is not always the case for all volcanoes. The particle size range and components of  
166 VA depend on eruptive processes, and hence are largely unpredictable. Typically, silicic (SiO<sub>2</sub>,  
167 >63% by weight) ash compositions produce more highly explosive eruptions, higher eruption  
168 columns, and finer VA particles (with very fine ash proportions of 30 to > 50%, compared to 1-  
169 4% of basaltic eruptions, Rose and Durant, 2009), leading to longer atmospheric residence times  
170 and wider dispersal of VA, although particle shape also influences the atmospheric lifetime of  
171 VA. After an eruption has occurred, some compositional information can be derived from

172 satellite measurements (Gangale et al., 2010; Clarisse et al., 2010a, 2010b, 2013), or in rare cases  
173 from direct airborne sampling of volcanic plumes (e.g., Rose et al., 2000). Hyperspectral infrared  
174 (IR) satellite measurements can distinguish VA from other airborne particulates (e.g., desert dust,  
175 wildfire smoke; Clarisse et al., 2010a; 2013) and can identify VA composition based on silica  
176 content (e.g., distinguish basaltic ash from rhyolitic ash; Gangale et al., 2010; Clarisse et al.,  
177 2010a). Ultraviolet (UV) satellite observations can potentially provide information on the iron  
178 oxide species present in VA (Carn and Krotkov, 2016; Go et al., 2022). However, satellite  
179 sensitivity to VA (and aerosol type in general) is limited, so ash plumes usually cannot be  
180 tracked very far from the source unless particle concentrations are rather high.

181         Critical for this review, the iron and phosphorus in VA has been suggested to impact  
182 ocean biogeochemistry (Langmann, 2013; Langmann et al., 2010; Duggen et al., 2007; Olgun et  
183 al., 2011, 2013). Studies have also shown that widely varying amounts and forms of bioactive  
184 metals (e.g., iron, zinc, cadmium) as well as toxic metals (e.g., lead, copper) and halogens (e.g.,  
185 fluorine, chlorine) can accompany VA. However, VA composition is highly dependent on both  
186 the volcano and the eruption, and more systematic studies of the compositions of ash are required  
187 (Langmann et al., 2010; Duggen et al., 2010; Frogner et al., 2001; Vogel et al., 2017; Shkinev et  
188 al., 2016; Koffman et al., 2021).

189         Volcanic eruptions are often difficult to forecast, although eruption ‘run up’ time and  
190 eruption magnitude are broadly correlated. Large-magnitude eruptions are typically preceded by  
191 weeks to months of increasing unrest, which can provide a warning of an impending eruption,  
192 although forecasting the timing and magnitude of an eruption remains challenging (Passarelli and  
193 Brodsky, 2012). The ability to forecast eruptions relies on ground-based monitoring data  
194 (seismic, ground deformation, gas emissions), which are not available for the vast majority of

195 volcanoes (Brown et al., 2015). While the ability of satellite observations to forecast the timing  
196 of volcanic eruptions is nascent (Poland and Anderson, 2020), satellite data are routinely used to  
197 assess volcanic emissions and impacts shortly thereafter (Poland et al., 2020).



198  
199 Figure 3. Conceptual diagram of 4 ash sizes (largest in yellow, followed by black, light green,  
200 and purple) with increasing distance from the volcano. Larger ash will be deposited in the  
201 immediate vicinity, and possibly dominate the mass flux of ash types compared to farther from  
202 the volcanic source where fine-sized ash and smoke remains. The pie charts represent the relative  
203 composition of ash in the ocean.  
204

205 Ideally, an atmospheric assessment of VA should include the following major  
206 components: 1) location and timing of eruption; 2) duration of volcanic activity; 3) determination  
207 of ash injection height; 4) area covered as the ash cloud disperses; 5) quantification of ash  
208 emission and dispersal; and 6) determination of ash plume mineralogical and chemical  
209 composition, physical properties, and changes in near-real-time. Current satellite technology can  
210 generally supply this information, but observational conditions and sensor limitations frequently  
211 work in combination to prevent successful detection. For example, the time of satellite overpass  
212 with respect to the eruption stage is critical because the initial plume's vertical extension  
213 provides the injection height, which in turn constrains the horizontal extension and dispersal of




































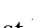

214 the volcanic cloud. When determining total aerosols in a satellite pixel using a passive sensor  
215 (e.g., MODIS or GOES/ABI, see Table 1), a clear sky view is needed so all the observed  
216 radiation can be linked to the aerosol loading. Partially cloudy scenes are frequently unused  
217 because of the inability to parse out the cloud from the aerosol contribution to the observed  
218 signal (see also Platnick et al., 2003). While geostationary sensors have been operational for a  
219 few decades and have been used to monitor historical eruptions (Holasek and Self, 1995;  
220 Marhese et al, 2014), these sensors lack adequate spatial and spectral resolution for  
221 quantification of fine aerosol loadings ( $<1 \mu\text{m}$ ). The poor sensor resolution of fine aerosols is  
222 important because these fine aerosols can travel the farthest, and thus are deposited over a very  
223 large area (Figure 3). The deployment of the latest generation of geostationary sensors has been  
224 a clear improvement with respect to this issue as the observations of the Himawari-8 Advanced  
225 Himawari Imager (AHI) and GOES-17 Advanced Baseline Imager (ABI, Table 1) enabled an  
226 excellent characterization of the vertical extension and evolution of the ash cloud of the 2022  
227 Hunga Tonga eruption (Carr et al., 2022). Furthermore, legacy and improved aerosol detection  
228 and retrieval algorithms (Pavolonis et al., 2015; Kondragunta et al., 2020, Gupta et al., 2019) are  
229 being ported to geostationary imagery, thus enabling aerosol information suitable for comparison  
230 with aerosol transport models. Satellite observations typically record less than 6% of the total  
231 erupted ash mass (Rose et al., 2001, their Table 7), and provide a biased sample of the grain size  
232 distribution (by preferentially providing measurements of fine sized ash ( $< 17 \mu\text{m}$ ) compared to  
233 what is observed on the ground ( $> 20 \mu\text{m}$ , Stevenson et al., 2015; Prata and Lynch, 2019). Satellite  
234 radiances may also be saturated by the strong VA signal immediately following an eruption, and  
235 satellite observations of VA mass are confounded by the VA composition unknowns (Krotkov et

236 al. 1999a). Both field and satellite measurements are needed to record the mass, distribution,  
237 composition, and other characteristics of the ash deposition (Cashman and Rust, 2020).

238         Regardless of observation sampling frequency, quantifying aerosols in the atmospheric  
239 column is an important challenge. Once emitted into the atmosphere, ash is transported  
240 horizontally and vertically within the atmosphere similar to any aerosol, and removed through  
241 either dry deposition (gravitational settling or turbulent deposition) or by wet deposition (by  
242 precipitation) out of the atmosphere (Mahowald et al., 2011a; Stohl et al., 2011). Understanding  
243 these transport processes is critical, not only to estimate the fetch of the deposition area, and also  
244 to elucidate the compositional chemical changes in the ash cloud during transit. The altitude of  
245 the plume is particularly important, because aerosols lofted higher will reside in the atmosphere  
246 longer. Particles reaching the stratosphere will have a much longer lifetime, as the stratosphere is  
247 more stable and does not have wet deposition processes (Stohl et al., 2011). While volcanic  
248 aerosols are present through the column in the immediate vicinity of the volcano, rapid  
249 sedimentation within a few hundred kilometers results in a volcanic cloud located in the mid to  
250 upper troposphere, on top of a ‘cleaner’ lower atmosphere. Thus, a significant portion of total  
251 aerosols (all aerosols, not just from volcanoes) are in the marine boundary layer immediately  
252 downwind from the volcano, where maximum deposition will occur.

253 Table 1. Assessment of historical, current, and future satellite missions, their period of  
254 performance, spatial and spectral resolution, and applicability to studying atmospheric and  
255 marine aspects of VA in coastal ecosystems. Satellites are colored by their capabilities (orange =  
256 land/air properties, blue = ocean ecosystem properties) to guide a quick look at what resources  
257 are available. Aerosol concentration and particle size can be obtained from aerosol optical depth  
258 and the Angstrom coefficient, and aerosol composition or aerosol type (VA versus others) is  
259 given by ultraviolet absorption, infrared emissivity, and backscattering polarization. The location  
260 of aerosols in the atmospheric column is given by lidar backscattering coefficients, ultraviolet  
261 absorption and emissivity in the infrared. In the water column, chlorophyll, particle load, and  
262 dissolved material can be retrieved through remote sensing reflectance inversion algorithms in  
263 the visible range. Particle load and phytoplankton carbon can be obtained from lidar  
264 backscattering coefficients. Acronyms: Advanced very-high-resolution radiometer (AVHRR),

265 Total Ozone Mapping Spectrometer (TOMS), Sea-viewing Wide Field-of-view Sensor  
266 (SeaWiFS), Advanced Spaceborne Thermal Emission and Reflection Radiometer (ASTER),  
267 Moderate Resolution Imaging Spectroradiometer (MODIS), Multi-angle Imaging  
268 SpectroRadiometer (MISR), Atmospheric Infrared Sounder (AIRS), Spinning Enhanced Visible  
269 and Infrared Imager (SEVIRI), Ozone Monitoring Instrument (OMI), Infrared Atmospheric  
270 Sounding Interferometer (IASI) on Meteorological Operational Satellite (MetOp), Cloud-  
271 Aerosol Lidar with Orthogonal Polarization (CALIOP) on the Cloud-Aerosol Lidar and Infrared  
272 Pathfinder Satellite Observation mission (CALIPSO), Global Ozone Monitoring Experiment-2  
273 (GOME-2), Geostationary Ocean Color Imager (GOCI) on the Communication, Ocean, and  
274 Meteorological Satellite (COMS), Visible Infrared Imaging Radiometer Suite (VIIRS) on Suomi  
275 National Polar-orbiting Partnership (SNPP), National Oceanic and Atmospheric Administration  
276 satellites (NOAA), Advanced Technology Microwave Sounder (ATMS), Ozone Mapping and  
277 Profiler Suite (OMPS), Advanced Himawari Imager (AHI), Earth Polychromatic Imaging  
278 Camera (EPIC) on Deep Space Climate Observatory (DSCOVR), Advanced Baseline Imager  
279 (ABI) on Geostationary Operational Environmental Satellites (GOES), Ocean and Land Colour  
280 Instrument (OLCI), Tropospheric Monitoring Instrument (TROPOMI), Geostationary  
281 Environment Monitoring Spectrometer (GEMS) on Geostationary-Korea Multi-Purpose  
282 Satellite-2 (GEO-KOMPSAT 2), Ice, Cloud, and Land Elevation Satellite 2 (ICESat-2), Earth,  
283 Cloud, Aerosol, and Radiation Explorer (EarthCARE), Ocean Color Instrument (OCI), Spectro-  
284 Polarimeter for Planetary Exploration (SPEXone), Hyper-Angular Rainbow Polarimeter-2  
285 (HARP-2) on Plankton, Aerosol, Cloud, ocean Ecosystem (PACE) satellite, Geostationary  
286 Littoral Imaging and Monitoring Radiometer (GLIMR) instrument.  
287

<b>Instrument</b>	<b>Mission</b>	<b>Resolution</b>	<b>Wavelengths</b>	<b>Capability</b>
* = geostationary	<b>Timeline</b>	(pixel length, km)	<b>(bold is hyperspectral, else multispectral)</b>	
AVHRR	1978 - present	1.1	Visible (green, red), NIR to IR	
TOMS (NIMBUS-7, Earth Probe)	1978 - 2005	4.7	UV	
Landsat-5,7,8,9	1984 - present	0.1	Visible, NIR to IR	 
SeaWiFS	1997 - 2010	1.1	Visible, NIR	 
ASTER (Terra)	1999 - present	0.015	Visible (green, red), NIR, TIR	
MODIS (Terra, Aqua)	1999/2002-present	1	Visible, NIR, IR	 
MISR (Terra)	1999 - present	4	Visible, NIR	
AIRS (Aqua)	2002 - present	13.5	<b>NIR, IR</b>	
SEVIRI (MSG)	2002 - 2022	3	Visible, NIR, IR	
OMI (Aura)	2004 - present	13 x 24	<b>UV – Visible</b>	
MetOp/IASI	2006 - present	1	<b>IR</b>	
CALIOP (CALIPSO)	2006 - present	5	Polarized lidar 2 channels: 532, 1064 nm	 
GOME-2 (MetOp-A)	2006 - present	40	<b>UV, Visible</b>	
GOCI (COMS*)	2010 - present	0.5	Visible and 1 NIR	 
VIIRS (SNPP, NOAA-20, NOAA-21)	2011 - present	0.375-0.75	Visible, NIR, IR	 
ATMS (SNPP, NOAA-20, NOAA-21)	2011 - present	15.8	Microwave radiances (23.8 – 183.3 GHz)	
OMPS (SNPP, NOAA-20, NOAA-21)	2011 - present	50	<b>UV</b>	
AHI (Himawari-8,9*)	2014 - present	0.5-4	Visible (blue, green, red), NIR, IR	
EPIC (DSCOVR)	2015 - present	18	UV, Vis, NIR	
ABI (Goes-16/17*)	2016 - present	2	Visible, NIR, IR	
OLCI (Sentinel 3a,b)	2016 - present	0.3	Visible, NIR	 
TROPOMI (Sentinel 5p)	2017 - present	3.5	UV, Visible, NIR	
GEMS (GEO-KOMPSAT 2B*)	2020 - present	0.5 - 2	<b>Visible, NIR</b>	 
ICESat-2	2018 – present	0.5 - 3	Elastic lidar, 532 nm	
EarthCARE	2023 launch date		Polarized UV lidar, Visible, NIR, IR, TIR	
OCI / SPEXone / HARP-2 (PACE)	2024 launch date	1	<b>UV, visible, NIR, IR</b> , with polarimeters	 
GLIMR	2026/7 launch date	0.3	<b>UV, NIR, IR</b>	 

288  
289

290           Satellite data are commonly used within models to better contextualize and forecast VA  
291 dispersion. Generally speaking, the study of volcanic ash transport makes use satellite data in  
292 different ways depending on the intended application (climate or biogeochemical or disaster  
293 response) and the nature of the model (Lagrangian or Eulerian types). Lagrangian type of  
294 transport models are generally preferred for rapid response because they can be quickly  
295 initialized with weather forecast information as well as satellite data that can be quickly  
296 processed (Gouhier et al, 2022). Thus, for example, initial satellite estimates of volcanic  
297 plume height (Chai et al, 2017) and total aerosol mass concentration amounts are used to  
298 initialize and constrain the forecast (Pardini et al, 2020). Satellite data are also used for  
299 verification and calibration of forecasts (Crawford et al,2022, Tadini et al, 2022, de Leeuw et

300 al, 2021). For climate applications, Eulerian modeling approaches are preferred for  
301 hemispherical or global simulations that encompass multiple eruptions and/or long time  
302 periods. They also either assimilate satellite to constraint simulations or are used to verify or  
303 adjust parameterizations assumed in the simulations (Wells et al, 2023; Bruckert et al, 2022;  
304 Muser et al, 2020)

305 In addition to the unknown composition of the material initially released to the  
306 atmosphere, the uncertainty of simulated aerosols in Earth system models are primarily due to: 1)  
307 the altitude of the volcanic plume, which depends on the eruption explosivity, ejected material  
308 density, entrainment, and gas temperatures; and 2) the particle size of ash falling out of the  
309 plume (Stohl et al., 2011). Note that there is a difference in language between volcanologists  
310 and the aerosol community, where the aerosol community uses ‘fine’ and ‘coarse’ for aerosols  
311 less than 2.5  $\mu\text{m}$  and 10  $\mu\text{m}$  in diameter respectively (Mahowald et al., 2011b), while the  
312 volcanic community considers ‘fine ash’ to be ash less than  $\sim 100 \mu\text{m}$  in size (e.g., Osman et al.,  
313 2020). In all cases, relatively larger ash particles will be removed much more quickly from the  
314 atmosphere due to gravitational settling (Petroff and Zhang, 2010). Consequently, as the plume  
315 moves downwind, the particle size distribution and relative composition of ash will change  
316 (Figure 3). The higher deposition of VA near a coast does not necessarily mean that open ocean  
317 areas are unaffected, particularly if VA is carried by strong offshore winds (Hamme et al., 2010).  
318

### 319 **3. Ash geochemistry in water**

#### 320 *Deposition and dissolution*

321 There are a number of known processes that can impact the spatiotemporal variability of  
322 phytoplankton response, including wet and dry deposition to marine surface waters, fluvial

323 inputs of terrestrial ash, sinking of ash particles in the water column, composition of ash  
324 leachates, and the role of organic compounds in facilitating elemental transfer and solubility  
325 (Figure 2). Taken together, these processes will direct future work to permit a detailed  
326 understanding of when and where VA inputs will have the greatest effect on marine primary  
327 productivity, and whether these inputs will be advantageous or deleterious to phytoplankton  
328 growth. Ultimately, satellite remote sensing offers very little in the realm of aqueous ash  
329 geochemistry, but understanding the pathways of ash dissolution in seawater can help improve  
330 and contextualize satellite observations, especially when ancillary in situ observations may be  
331 available.

332         Ash constituents can become solubilized or otherwise available to phytoplankton  
333 communities through several pathways: 1) dissolution of dry ash particles that are deposited  
334 directly to surface waters (dry deposition), 2) dissolution of ash aerosols in clouds or humidity  
335 prior to deposition via rain or snowfall to surface waters (wet deposition, and note that wet  
336 deposition does not always include ash dissolution), or 3) redistribution of ‘fossil’ ash that was  
337 previously deposited on terrestrial landscapes via either wind remobilization or rainfall-runoff  
338 processes and riverine transport. Leaching experiments (to solubilize away materials with water)  
339 conducted over the last few decades indicate that VA is a consistent and significant source of  
340 nutrients, essential elements, and trace metals, including Fe, Al, P, F, Mn, Zn, Cl, Ca, K, Mg, Na,  
341 and SO<sub>4</sub> (Witham et al., 2005; Duggen et al., 2010; Stewart et al., 2020). Similar enrichments of  
342 metals have been observed immediately post-eruption in ash-impacted seawater (Censi et al.,  
343 2010) and dissolution is suggested to occur fast enough to support enhanced primary production  
344 in surface waters prior to sinking of ash particles (Frogner et al., 2001). Although it has not been

345 measured directly, VA may be reemitted from surface waters to the overlying atmosphere, as has  
346 been observed for dust (Cornwell et al., 2020).

347         Chemical composition, solubility, and particle size of VA vary widely (Duggen et al.,  
348 2007; Olgun et al., 2013; Hoffman et al., 2012; Mahowald et al., 2018). Fresh, dry VA hosts  
349 myriad soluble elements, most notably Fe for nutrient-limited seawater, that quickly dissolve in  
350 water vapor (humid environments) or are washed away by meteoric water (rainfall, rivers, etc.)  
351 upon initial water-ash interactions (Duggen et al., 2010). Some of these elements may be in the  
352 form of sulfate and halide salts, which may form at magmatic temperatures (600–1200 °C),  
353 through chemisorption near the condensation temperature of sulfuric acid (~200 °C) in plumes,  
354 or possibly through partial dissolution of ash in contact with sulfuric and halogen acids at lower  
355 temperatures (Delmelle et al., 2018). While the formation of Fe-sulfate salts has not been  
356 observed, their existence has been invoked to explain the rapid release of Fe upon contact with  
357 water (Ayris and Delmelle, 2012). Since the dissolution of volcanic salts in clouds and water  
358 vapor occurs at a lower pH than seawater, the solubility and potential bioavailability of some  
359 elements, such as Fe, may be significantly enhanced during wet deposition compared to dry  
360 deposition (Duggen et al., 2010). Finally, larger VA aggregates, which are promoted by high  
361 humidity, enhance deposition of ash particles in surface waters closer to the eruption site because  
362 atmospheric residence time and distance traveled are a function of particle size (Duggen et al.,  
363 2010; Colombier et al., 2019).

364         During volcanic eruptions, a portion of ash is deposited on terrestrial landscapes. Due to  
365 the physicochemical nature of deposited ash (e.g., organo-metallic complexes, low pH, presence  
366 of toxic metals), VA soils have been shown to stabilize large stocks of organic carbon (Eswaran  
367 et al., 1993; Tonneijck et al., 2010). The reaction of volcanic gases with ash and water vapor

368 results in soluble salts from freshly deposited ash, and could lead to acute effects in proximal  
369 freshwater environments (Smith et al., 1982; Modenutti et al., 2013), as well as potentially  
370 chronic impacts on coastal environments over the long term. Although fossil volcanic ash has  
371 lost most of its salt coating during first contact with water, the disaggregation of previously  
372 deposited ash particulates (during river or wind transport, debris flows, human activity, etc.) has  
373 been shown to enhance the release of elements such as Ca, Na, Al, K, and Si to exposed waters  
374 (Genareau et al., 2016). On a macroscale, volcanic eruptions significantly alter watershed  
375 hydrology and geomorphology via soil destabilization, accumulation of dead woody debris, and  
376 deposition of new ash layers (Pierson and Major, 2014). Taken together, these hydrogeomorphic  
377 changes result in massive and stochastic delivery of organic carbon and pyroclastic material to  
378 coastal regions (Mohr et al., 2017; Umazano and Melchor, 2020). The legacy effects of volcanic  
379 events can persist for decades to centuries after the eruption occurs (Pierson and Major, 2014;  
380 Steinman et al., 2019; Major, 2020). This phenomenon is recorded in sedimentary records, which  
381 indicate that deposited ash enhances organic carbon burial and preservation in coastal sediments  
382 on historic and geologic timescales (Lee et al., 2018; Longman et al., 2019). These impacts result  
383 from a combination of fertilization and enhanced primary production in surface waters, oxygen  
384 depletion in ash-affected sediments, and direct organo-mineral associations (Haeckel et al., 2001;  
385 Hembury et al., 2012; Longman et al., 2021).

386         Regardless of whether VA enters marine surface waters fresh or aged, and via wet or dry  
387 deposition, previous studies agree that the presence of adsorbed organic ligands (any molecule or  
388 atom that binds to a receiving molecule) during transport further enhances the solubility and  
389 mobilization of some elements from VA (Duggen et al., 2010; Censi et al., 2010). It is suggested  
390 that these organic ligands may derive from phytoplankton, cell lysis, and/or bacterial

391 decomposition of organic matter in surface seawater or originate from burnt vegetation or  
392 volcanic gases in eruption plumes (Randazzo et al., 2009; Baker and Croot, 2010; Taylor and  
393 Lichte, 1980; Capaccioni and Mangani, 2001). Although organic ligand-metal interactions  
394 appear to be a major factor in VA solubility and bioavailability, very little is known about how  
395 organic carbon may adsorb onto fresh VA during transport (Weinbauer et al., 2017), let alone its  
396 leachability and contribution to dissolved organic carbon in ash-affected seawater. A water  
397 quality study of the effects of a volcanic eruption on Patagonian lakes showed up to an 8-fold  
398 increase in total suspended solids concentration, but no change in dissolved organic carbon  
399 concentration (Modenutti et al., 2013), which suggests that bulk dissolved organic carbon inputs  
400 from ash deposition may be negligible in marine environments. Further research on the content  
401 and composition of organic carbon associated with VA is needed.

402         The aging of VA between initial eruption and subsequent deposition to surface seawater  
403 appears to be a major control on the potential beneficial, harmful, or neutral impacts on marine  
404 phytoplankton and higher trophic levels. Several studies have shown that the composition of ash  
405 collected immediately following an eruption can change during laboratory storage, such that  
406 older (unhydrated) samples release less Fe during leaching experiments than fresher samples  
407 from a similar volcanic setting (Jones and Gislason, 2008; Duggen et al., 2010; Olgun et al.,  
408 2011). This decreased Fe solubility over a period of 10–25 years has been attributed to the loss of  
409 soluble salt coatings on ash grain surfaces, although this loss has not been observed directly.

410         In contrast, the environmental aging of VA, wherein ash remains on the land surface for  
411 years to centuries following an eruption and interacts with meteoric and groundwater subsequent  
412 to remobilization by wind or water, also impacts ash geochemistry and may enhance the  
413 bioavailability of Fe and other metals in ways unrelated to salt coatings. For instance, in the

414 high-precipitation environment of southern Alaska, environmental aging processes resulted in 5x  
415 higher Fe solubility and 10x higher easily-reducible Fe compared to fresh, dry-deposited ash  
416 (Koffman et al., 2021). Changes in Fe-bearing phases may relate to soil formation processes and  
417 the migration of Fe through the ash/soil profile through time (Koffman et al., 2021), and thus  
418 aging processes are likely to differ depending on climate regime. Wind remobilization events in  
419 volcanically-active regions (Flower and Kahn, 2017) have been documented following eruptions  
420 in Iceland, Alaska, Kamchatka Peninsula and Patagonia (Bullard et al, 2016, Meinander et al,  
421 2022 and references within), so further work is needed to determine the role of ash  
422 remobilization events in providing nutrients to ocean ecosystems, particularly considering how  
423 aging processes may enhance or reduce the solubility of Fe and other bioactive metals.

#### 424 **4. Ash impacts on ocean biota**

##### 425 *4.1 Toxicity*

426 In addition to fertilization impacts on ecosystems, VA has the potential to deliver toxic  
427 quantities of trace metals and halogens to the environment (Kockum et al., 2006) and may also  
428 scavenge anthropogenic organic compounds such as dioxins, polychlorinated biphenyls (PCBs)  
429 and polycyclic aromatic hydrocarbons (PAHs) (Ayris and Delmelle, 2012, and refs therein).  
430 Phytoplankton toxicity has been reported for Cu concentrations of 11–200 ppm in seawater  
431 (Mann et al., 2002), for Pb concentrations of 20–465 ppb, and for Cd of 0.23–500 ppb  
432 (Echeveste et al., 2012). Other trace metals found in VA may also be toxic at high  
433 concentrations. While desert dust is recognized as the largest natural source of Cu to the ocean  
434 surface (Lopez et al., 2019) and has been found to cause toxic effects (Paytan et al., 2009),  
435 explosive volcanic eruptions can deliver much greater quantities of Cu and other metals to  
436 relatively small geographic areas, thus increasing concentrations above toxic thresholds. For

437 instance, using measurements from Aleutian Arc volcanoes, Koffman et al. (2021) estimated that  
438 an eruption with a similar magnitude to Kasatochi (2008) could deposit ~1400–2600 metric tons  
439 of Pb, ~9000–18,000 metric tons of total Cu, and 400–800 metric tons of soluble Cu in nearby  
440 waters. These estimates are somewhat higher than those for the 2008 eruption of Chaitén, likely  
441 reflecting differences in volcanic composition (Ruggieri et al., 2012). While it seems plausible  
442 that VA deposition could have widespread negative impacts on marine ecosystems, to our  
443 knowledge this effect has not been observed, perhaps due to rapid physical transport (dilution) in  
444 ocean waters.

445 Toxicity depends on the amount of free, uncomplexed metal available; as organic ligand  
446 concentrations increase, metal uptake by transport proteins decreases (Sunda and Huntsman,  
447 1998). Therefore, toxicity can only occur once available chelators (chemical compounds binding  
448 to metal ions) are saturated (Moffett et al., 1997). In terms of Cu toxicity, cyanobacteria are the  
449 most sensitive, dinoflagellates and coccolithophores have intermediate tolerance, and diatoms  
450 have the highest tolerance (Lopez et al., 2019). Toxicity sensitivity scales with cell size (where  
451 larger cells have higher tolerance), possibly due to diffusion rate differences (e.g., Behrenfeld et  
452 al., 2022) across cell sizes. Elevated trace metals from VA deposition can impact phytoplankton  
453 species differently, and these differing responses can lead to shifts in community composition  
454 (Hoffman et al., 2012). It may be expected that ongoing ash inputs in volcanically active regions  
455 play a role in driving community structure, and future satellites with higher spectral resolution  
456 like NASA’s PACE (Plankton, Aerosols, Clouds, and ocean Ecosystem; Werdell et al., 2019)  
457 mission may help in observing community composition changes following ash deposition due to  
458 the improved information about phytoplankton communities found in hyperspectral data (e.g.,  
459 Chase et al., 2017; Kramer et al., 2022).

460 As well as delivering large quantities of metals to the environment, volcanoes emit  
461 halogens such as Br<sup>-</sup> and F<sup>-</sup> that are known to cause severe toxic effects to humans, livestock,  
462 and both terrestrial and aquatic ecosystems. Emissions of hydrofluoric acid from the 1783–1784  
463 Laki eruption (Iceland) decimated livestock and caused long-term health problems such as  
464 fluorosis (Thordarson and Self, 2003), which is a skeletal and dental disease arising from  
465 overexposure to fluoride. Fluorosis in both wild and domesticated herbivore populations has  
466 been observed following recent eruptions in Chile (Flueck, 2016). Fluoride can be toxic to  
467 aquatic organisms at high concentrations (Camargo, 2003), but little is known about the impacts  
468 of volcanic fluoride emissions on marine ecosystems. Additional work is needed to understand  
469 the potentially toxic impacts of volcanic eruptions. Satellite imagery cannot directly observe  
470 toxicity, but satellites could, for instance, observe the impact of toxicity via low phytoplankton  
471 concentrations compared to what is expected for similar light, nutrient, and zooplankton levels.

#### 472 *4.2 Phytoplankton*

473 The observed impacts of VA on marine organisms are scarce and while the response of  
474 phytoplankton is the most commonly reported, these results vary (Figure 1). As previously  
475 discussed, while VA in seawater may provide limiting and co-limiting nutrients needed for  
476 phytoplankton to grow, VA may also contain toxic metals that inhibit phytoplankton growth.  
477 Diffusion rates of nutrients or metals from VA into seawater will vary with VA characteristics,  
478 namely size and solubility. VA may have no effect whatsoever on phytoplankton growth; the ash  
479 can be diluted in seawater depending on local physical conditions, there may be a lack of nutrient  
480 availability in the ash, and/or the phytoplankton may not be nutrient-limited, all of which could  
481 lead to no change in phytoplankton growth rate. Regardless of the nutrients contained in ash, the  
482 addition of highly absorbing material (both particulate and dissolved ash) can alter the light

483 environment, reducing the light available for photosynthesis. In all cases, some phytoplankton  
484 groups may have advantages that allow them to perform better than others in ashen seas  
485 (Hoffman et al., 2012, Kramer et al., 2020). One case study, which analyzed stream water quality  
486 during and after the 2011 eruption of Mount Bulusan (Philippines), showed a 2-fold increase in  
487 mean silica concentration that is thought to have caused an observed shift toward a diatom-  
488 dominant community in the estuary into which the streams drain into (Siringan et al., 2018).  
489 Changes in phytoplankton community composition following VA input may also alter the  
490 structure of the marine food web across trophic levels (see the following sections). High  
491 concentrations of ash can also dilute the food source for zooplankton and/or clog fragile mucous  
492 membranes (see Drazen et al., 2020 and refs therein), which could relieve top-down grazing  
493 pressures on phytoplankton and allow cells to accumulate. The challenge of distinguishing such  
494 biological responses becomes even more complex when the uncertainty of satellite observations  
495 used to derive phytoplankton properties is taken into consideration.

496         Methods to assess the biological response to different ash additions include both in situ  
497 bottle incubation studies as well as remote sensing methods (e.g. Hoffman et al., 2012 vs.  
498 Duggen et al., 2007). It is difficult to time a research cruise to be simultaneous with an extreme  
499 and unpredictable event such as a volcanic eruption in order to assess the ash effect directly  
500 (Bisson et al., 2020a), and thus remote sensing is an excellent tool for looking at ocean  
501 responses. A primary challenge of assessing biological effects of ash from satellite remote  
502 sensing is that no satellite offers direct observations of phytoplankton. Rather, ocean color  
503 satellites measure top-of-atmosphere reflectance, which requires appropriate atmospheric  
504 correction to uncover the ocean signal (remote sensing reflectance), and remote sensing  
505 reflectance covaries with phytoplankton, non-algal particles (ash, detritus, sediment), and colored

506 dissolved organic matter that may be enhanced by ash leachate. For most of the ocean, satellite  
507 chlorophyll-a is derived from empirical algorithms using remote sensing reflectance. In these  
508 waters, phytoplankton (and co-varying constituents) drive the ocean color signal. However,  
509 phytoplankton alone do not drive the ocean color signal when ash is present, and ash is optically  
510 complex, as it spans different sizes, solubilities, and composition (Kramer et al., 2020). In these  
511 waters, the standard chlorophyll-a algorithm likely does not perform accurately. Several studies  
512 have explored an oceanic response to ash using satellite observations of chlorophyll-a (a pigment  
513 common to all phytoplankton; Duggen et al., 2007, Hamme et al., 2010, Henson et al., 2013,  
514 Browning et al., 2015, Westberry et al., 2019) because chlorophyll-a can be derived from remote  
515 sensing reflectance. However, chlorophyll-a is an imperfect metric for phytoplankton biomass, as  
516 pigment concentration and expression vary with changes in phytoplankton physiology (by up to  
517 a factor of ~3, see Behrenfeld et al., 2005 and data therein), and the presence of VA in the ocean  
518 and atmosphere affects the performance of satellite algorithms used to obtain accurate  
519 chlorophyll-a estimates. Westberry et al (2019) also considered the response of chlorophyll-a  
520 fluorescence and phytoplankton carbon to study changes in growth/physiology for two volcanic  
521 eruptions, but these products (and any products derived from remote sensing reflectance  
522 inversions, including phytoplankton absorption) may also be sensitive to ash in the water and/or  
523 atmosphere. Ultimately, chlorophyll-a, fluorescence or phytoplankton carbon may not be the  
524 most useful metric to quantify planktic ecosystem changes because changes in chlorophyll  
525 cannot be explicitly linked to different types of phytoplankton (including harmful algal species,  
526 which are of particular concern for human health and fisheries). To develop a holistic perspective  
527 on volcanic ash impacts, remote sensing observations coupled with shipboard measurements are  
528 needed.

529 Little research has been conducted to quantify the optical influence of ash on remote  
530 sensing reflectance, but available work suggests that rhyolitic ash in seawater biases satellite  
531 chlorophyll-a by more than an order of magnitude for oligotrophic waters, and by less than a  
532 factor of 2 for environments with  $> 0.5 \text{ mg chlorophyll-a m}^{-3}$  (Browning et al., 2015). A recent  
533 study found different inherent optical properties (enhanced absorption by dissolved material in  
534 particular) during Thomas Fire ash deposition (Kramer et al. 2023). There are substantial  
535 knowledge gaps in understanding how VA affects inherent optical properties of seawater. One  
536 reason for the knowledge gap is in part because remotely sensed inherent optical properties are  
537 retrieved from apparent optical properties, and quantifying the latter is highly uncertain during  
538 VA deposition. The ash particles present in the atmosphere act as strong light-absorbing  
539 aerosols, and the standard ocean color atmospheric correction algorithms may not fully remove  
540 this component, resulting in an enhanced water-leaving signal that translates to an augmented  
541 chlorophyll-a signal (Gordon & Wang 1994; Nobileau & Antoine 2005; Ahmad et al. 2010).  
542 More work in this area is needed, especially because the relative uncertainties associated with  
543 satellite-derived chlorophyll-a concentrations are a function of both the ocean environment and  
544 the ash type. Despite these challenges and those mentioned above, satellite remote sensing  
545 remains an important tool for studying the biological effect of ash in situ, because satellite  
546 observations can provide time-series context while also resolving spatial heterogeneity in the  
547 ocean signal. Improved quantification of uncertainties in the remote sensing signal will  
548 undoubtedly improve interpretation of any biological response in the ocean to VA input.

#### 549 *4.3 Zooplankton and Fish*

550 One blind spot of remote sensing is the quantification of VA impact on zooplankton,  
551 which feed on phytoplankton and are a link to higher trophic levels, including fish. Although

552 detecting zooplankton through remote sensing platforms is in development (e.g., Behrenfeld et  
553 al., 2019, Basedow et al., 2019), existing satellite observations can be coupled with in situ  
554 zooplankton observations to be used in food-web models for improved prediction of herbivory  
555 rates (e.g., Bisson et al., 2020b). At the time of writing, there are no studies that characterize the  
556 effects of VA on marine zooplankton. An analogy may be found in lake zooplankton, where one  
557 study in the Andean North-Patagonian lakes found that filter feeders (mainly cladocerans) did  
558 not reach adulthood when VA concentration exceeded 8 mg L<sup>-1</sup> (Balseiro et al., 2014), and in  
559 general, survival and fecundity decreased following ash exposure. This study noted the  
560 resurgence of zooplankton in the year following the eruption, implying a short-term effect.  
561 Parallels may also be drawn from the deep-sea community, through studies of nepheloid layers  
562 and sediment resuspension events. Increased sensitivity of zooplankton to ash concentration with  
563 distance from the coast might be expected, as these open ocean organisms are likely adapted to  
564 water without high sediment concentrations. Physiological distress can be caused by ash  
565 clogging the respiratory and olfactory membranes of these animals, and sediment can reduce the  
566 buoyancy of gelatinous plankton if it adheres to them (Drazen et al., 2020, Robison, 2009). Filter  
567 feeders may experience bottlenecks within their fragile mucous nets as well as dilution of food  
568 due to ash in seawater. More work is needed to quantify the extent to which ash affects  
569 zooplankton based on the expected range of ash concentrations and the associated zooplankton  
570 response, especially to inform coastal communities of possible ecological changes in the  
571 nearshore environment.

572 Light is a primary factor in structuring the distribution of marine organisms in the upper  
573 ocean, including zooplankton and fish, and light moderates predator-prey interactions between  
574 the two (Hansen and Visser, 2016). Remote sensing reflectance, photosynthetically available

575 radiation (PAR), and light attenuation are all measured routinely from satellites. Ash deposition  
576 onto the ocean surface has the potential to decrease light levels (i.e., lower PAR, higher light  
577 attenuation) by increasing turbidity, a factor known to alter predator-prey dynamics due to its  
578 impact on visual predators (Utne-Palm, 2002, Pangle et al., 2012). Diel vertical migration is a  
579 ubiquitous behavior during which many zooplankton and fish species migrate from the surface  
580 ocean, where they feed at night, to deeper, darker waters during the day, thereby decreasing the  
581 likelihood of predation by such visual predators. This substantial migration of biomass is  
582 controlled largely by modulations in surface light levels (Cohen and Forward, 2009) and results  
583 in the active transport of carbon and other nutrients from the sea surface to depth - an important  
584 part of the ocean's biological carbon pump (reviewed in Steinberg and Landry, 2017). A strong  
585 negative relationship has been documented between zooplankton vertical migration depth and  
586 light attenuation; in this case, increased turbidity led to a shallower migration depth (Ohman and  
587 Romagnan, 2016). Similar effects were found in Lake Tahoe, when wildfire smoke and ash  
588 increased turbidity and decreased migration depth (Urmy et al., 2016). While untested for ocean  
589 systems, we hypothesize that the deposition of VA would alter vertical migration behavior,  
590 thereby temporarily impacting predator-prey dynamics, and the active transport of carbon by  
591 migrating biota. Future work with lidar satellites in combination with ocean color measurements  
592 may help address these predator-prey dynamics from space (Behrenfeld et al. 2019).

593         Most of the studies of VA and higher marine trophic levels (e.g., fish) come from just  
594 two eruptions: Mt St Helens in 1980, and Kasatochi in 2008. Experiments using the ash from the  
595 Mt St Helens eruption on juvenile and salmonid smolts (Newcomb and Flagg, 1983) and Pacific  
596 herring larvae (Boehlert and Morgan, 1985) reached different conclusions. While VA was found  
597 to be detrimental to salmon smolts at high concentrations (Newcomb and Flagg, 1983), it

598 increased the feeding rate of Pacific herring larvae (Boehlert and Morgan, 1985). Both studies  
599 indicated that the particulate component of the ash impacted the fish, rather than any toxicity  
600 imparted from soluble components (Newcomb and Flagg, 1983, Boehlert and Morgan, 1985).  
601 These studies only considered the short-term effects of ash addition, over scales of less than a  
602 day. In contrast, studies of the impacts of the 2008 Kasatochi eruption focused on interannual  
603 timescales. The eruption of iron-rich ash over normally iron-depleted marine waters led to a  
604 phytoplankton bloom visible in satellite data, which was then used to explain higher salmon  
605 numbers the following year (Parsons and Whitney, 2012), although this result has been contested  
606 (McKinnell, 2013) and subsequently defended (Parsons and Whitney, 2014). The impact of ash  
607 on fish will also vary depending on the life stage of the affected species, as smaller juvenile fish  
608 are more vulnerable to toxins or dampened growth.

609         Beyond fish, VA deposition can impact other marine organisms. For instance, iron  
610 enrichment can favor phytoplankton species that are detrimental to coral reefs (Schils,  
611 2012). Thick ash deposition can also directly obliterate coral reefs (Vroom and Zgliczynski,  
612 2011) or lead to the loss of shallow water habitat (Zimmermann, Ruggerone et al. 2018). Further  
613 work, including ongoing remote sensing developments for coral reefs (Hedley et al., 2016) is  
614 needed to determine the range of beneficial, negative, or neutral impacts on higher trophic levels  
615 and on other aspects of marine ecosystems.

## 616 **5. Recommendations for future work**

617         Future volcanic eruptions and other VA ash deposition events in coastal areas need to be  
618 monitored from a multitude of perspectives, and remote sensing data can contribute in a number  
619 of different ways. Here we summarize six key considerations, pointing to future research  
620 directions that will make the most of satellite data for exploring biological signals in the wake of

621 VA deposition. First, the remote sensing reflectance used to derive chlorophyll-a is only as good  
622 as the atmospheric correction algorithms used to produce it, and even routine errors in  
623 atmospheric correction can influence the magnitude of derived chlorophyll-a (e.g., Siegel et al.,  
624 2000, Feng and Hu, 2016, Bisson et al., 2021). Ash plumes introduce strongly absorbing aerosols  
625 into the atmosphere, and the standard ocean color atmospheric correction methods are not as  
626 accurate when such aerosols are present. Thus, an improved understanding of how ash affects  
627 atmospheric correction and the satellite chlorophyll-a product is urgently needed, especially to  
628 properly interpret satellite chlorophyll-a observations during and after volcanic  
629 eruptions. Examining the impacts of ash in seawater on remote sensing reflectance and on the  
630 inherent optical properties derived from satellite measurements will also improve the estimates  
631 of chlorophyll and other in-water properties from space.

632         Second, the timing of the eruption and availability of ‘clear’ (cloud-free) skies must be  
633 considered. Depending on the local ocean circulation patterns, ash may be retained or detrained  
634 from the system, and the relevant time and spatial scales of dispersion may need to be resolved  
635 more frequently in some systems than others (e.g., compare the California Current ecosystem  
636 with the North Pacific). Geostationary satellites can observe hourly changes in water  
637 characteristics, but they do not provide global coverage. There are two planned geostationary  
638 missions that will provide increased temporal (and spectral) coverage for US waters: NASA’s  
639 GLIMR satellite and NOAA’s GEO-XO satellite. It is also important to consider the long-term  
640 after-effects from volcanoes, including intermittent pulsing events (e.g., heavy rains that wash  
641 material into the ocean), or the slow flux of winds carrying terrestrially deposited VA into the  
642 ocean over time. Increasing the scales of observation over both space and time will allow for

643 higher-resolution sampling of the surface ocean following an ash deposition event, and ideally  
644 improve estimates of the impacts of VA on the system.

645 Third, passive remote sensing is limited in its ability to quantify the effect of ash on  
646 marine ecology and biogeochemistry because ash plumes and clouds associated with volcanic  
647 eruptions block the ocean radiance signal from detection by passive ocean color satellites,  
648 necessitating clear sky days for observing any ocean change. Active (lidar) satellites (e.g.,  
649 CALIOP, ICESat-2) have a smaller footprint (~10-100 m, Magruder et al., 2020, Markus et al.,  
650 2017) to detect ocean signals in gaps between and within thin clouds, making them useful tools  
651 for monitoring the marine response to ash deposition when passive ocean color satellites  
652 (typically 1 km pixel size) cannot retrieve a signal due to ash or cloud cover. However, lidar  
653 satellites do not measure chlorophyll-a, and instead measure particulate backscattering, which is  
654 an optical quantity that covaries with both phytoplankton and VA particles (and/or other ocean  
655 particulates). As such, lidar satellites will be useful to detect change, but it may be difficult to  
656 discern whether the change is due to the ash concentration or the phytoplankton concentration.  
657 Further in situ observations of the relationships between particle backscattering and VA particles  
658 in seawater may be useful for improving these relationships from space, especially by  
659 incorporating polarization properties (Collister et al., 2020, 2018) when available.

660 Fourth, VA needs to be sampled in near-real time, with a combination of close-to-vent  
661 fallout sampling with distal and in situ sampling inside the plume. Only through in situ sampling  
662 in real time will there be a complete analysis of the physicochemical properties needed for  
663 atmospheric modeling and satellite interpretation. Our understanding of volcanic events may be  
664 greatly enhanced by a planned and coordinated field response to the next large eruption, with  
665 efforts similar to the Nearshore Extreme Events Reconnaissance program (NEER,

666 <https://neerassociation.org>) and the COmmunity Network for Volcanic Eruption ResponSE  
667 (CONVERSE, <https://volcanoresponse.org>).

668 Fifth, further work is needed to reconcile satellite and ground-based observations of ash  
669 dispersal, which may be accomplished by matching known eruptions with available data from  
670 satellites (Table 1). Satellite retrievals sometimes provide smaller ash particle sizes than are  
671 observed in the field, and estimates of the location and amount of ash deposited differ between  
672 satellite measurements of ash clouds and tephra (fragmented material from volcanic eruption)  
673 mapping (Cashman and Rust, 2020). In order to resolve this discordance, one could focus a small  
674 pilot study on volcanoes with recurring activity, or those with available field data. In all cases,  
675 two major limitations are when 1) coastal volcanic eruptions do not coincide with offshore winds  
676 which would send ash over the ocean, and 2) satellite data are not available due to cloud cover or  
677 thick plumes. When satellite data are not available, additional remote sensing tools can help  
678 study the biological response of ash in situ, including Argo floats equipped with biological  
679 sensors (e.g., Mittal and Delbridge, 2019). Argo observations provide water column  
680 measurements that extend beyond what a satellite can ‘see,’ allowing the structure of the water  
681 column and changes to the mixed layer depth to be quantified (and occasionally euphotic layer  
682 depth for floats equipped with downwelling irradiance sensors). Other remote technologies can  
683 help, including gliders and drones equipped with radiometers, particularly if they are deployed  
684 downwind of active volcanoes.

685 Sixth, satellite observations can be used within models to extract more information than  
686 what is available from satellite data alone. For example, contextualizing satellite observations  
687 within atmospheric transport models can enable quantification of ash deposition rates.  
688 Thereafter, running regional physical ocean mixing models may help constrain residence times

689 and dilution rates of VA in seawater. Satellite observations used to drive ecological models may  
690 also be used to test hypotheses and diagnose whether derived rates are realistic or not, given  
691 prior information about the environment (Bisson et al, 2020a). Better quantifying the first-order  
692 impacts of VA on an ocean ecosystem will also allow for modeling studies to probe the  
693 cascading effects of a volcanic eruption, such as the implications for higher trophic levels or for  
694 carbon export via the biological pump.

695         Thanks to the increased satellite monitoring around the world in the last ~ 10 years, there  
696 is a better understanding of volcanic activity globally. While monitoring is still inadequate  
697 particularly at high latitudes, there are regions of interest where certain volcanoes exhibit  
698 frequent activity, making them candidates for increased monitoring or, if possible, dedicated  
699 intensive observational campaigns. A number of high latitude volcanoes in the Northern  
700 Hemisphere (e.g., Semisopochnoi, Great Sitkin, Gareloi, Cleveland, Pavlof, Sheveluch,  
701 Bezymianny, Chirinkotan, Kudryavy) exhibit frequent minor activity and are located upwind of  
702 ash sensitive ecosystems, so these volcanoes are possible candidates for enhanced monitoring.  
703 There are less active volcanoes of interest in the in the high latitude Southern Hemisphere,  
704 chiefly Mt Michael in the South Atlantic (emitting a plume nearly constantly over the last  
705 decade) and Piton de la Fournaise in Reunion Island. Autonomous platforms like Argo floats  
706 (equipped with optical sensors) operating downwind from these locations are a possibility for  
707 opportunistic studies.

708         At lower latitudes, there are volcanoes with frequent low activity and with visible low  
709 altitude plumes. These volcanoes include Kilauea, Nishina-shima, Etna, Barren Island, and  
710 several Andean and Galapagos islands volcanoes. Accessibility to these volcanoes is better than  
711 those at high latitudes, and clear sky views needed for satellite observations are more likely. The

712 lower latitude waters associated with these volcanoes may have different nutrient regimes than  
713 those of the high latitudes, enabling a spectrum of ash studies across environmental conditions.  
714 Finally, we also mention Icelandic volcanoes, as while they do not exhibit as frequent activity as  
715 the volcanoes listed, they are located in an area with very high surveillance and have the  
716 potential to be rapidly studied in situ due to their proximity to urban centers. Another interesting  
717 feature is the frequent and almost predictable blowout of aged ash in the southern Icelandic  
718 shores. This process deposits VA hundreds of kilometers into the open ocean. In general, Iceland  
719 presents a number of interesting logistical and scientific features that could be used to better  
720 understand the concept of aeolian deposition impacts in marine ecosystems.

721         To facilitate data synthesis as the remote sensing and ground truthing of satellite data  
722 continues to evolve, we encourage researchers to clearly state their assumptions (as different  
723 fields have different conventions), publish all relevant raw data calculations/codes following  
724 FAIR principles (i.e., Findability, Accessibility, Interoperability, Reuse), and scaling parameters  
725 used so measured fluxes, concentrations, rates, etc. can be refined over time instead of requiring  
726 a new eruption to conduct a new experiment. These approaches will promote data synthesis  
727 within and among disciplines as research on VA deposition and effects in the marine realm  
728 continue to evolve. Progress can also be made by looking outside volcanic eruptions into other  
729 types of stochastic environmental events that affect material transfer and ecological effects at the  
730 land-air-ocean interface (e.g., atmospheric deposition of dust and wildfire ash to surface waters).  
731 Although the geochemistry of material exported to coastal margins will not be the same as VA,  
732 in situ and remote sensing efforts to capture the environmental response to these events is similar  
733 to that of volcanic eruptions.

734

735 **Acknowledgements**

736 We are grateful to support and ideas from Laura Lorenzoni, Joel Scott, David Green, Toby  
737 Westberry, and Shanna McClain. This work was funded through a NASA TWSC grant  
738 80NSSC22K0049 to KMB. CM, BK, and KS were supported through the North Pacific Research  
739 Board (NPRB) 2101A. NMM, EG, and MEP were supported by the NASA Science Mission  
740 Directorate Interdisciplinary Science grant 80NSSC20K1674. SAC was supported by NASA  
741 Interdisciplinary Research in Earth Science grant 80NSSC20K1773.

742

743 **Description of author's responsibilities**

744 KMB led the writing with input from all authors. SG, NM, SW, BK, and SAC were leaders of  
745 different subgroups. KMB produced Figure 1, Figure 3, and Table 1. KS produced Figure 2. SD,  
746 EG, SK, NK, CM, MEP, KS, and CW contributed writing and final edits on the manuscript.

747 **References**

748  
749 Achterberg, E. P., Moore, C. M., Henson, S. A., Steigenberger, S., Stohl, A., Eckhardt, S., ... &  
750 Ryan-Keogh, T. J. (2013). Natural iron fertilization by the Eyjafjallajökull volcanic  
751 eruption. *Geophysical Research Letters*, 40(5), 921-926.

752  
753 Ahmad, Z., B. A. Franz, C. R. McClain, E. J. Kwiatkowska, J. Werdell, E. P. Shettle, and B. N.  
754 Holben. 2010. New aerosol models for the retrieval of aerosol optical thickness and normalized  
755 water-leaving radiances from the SeaWiFS and MODIS sensors over coastal regions and open  
756 oceans. *Appl. Opt.* doi:10.1364/AO.49.005545

757  
758 Ayris, P., & Delmelle, P. (2012). Volcanic and atmospheric controls on ash iron solubility: A  
759 review. *Physics and Chemistry of the Earth, Parts A/B/C*, 45, 103-112.

760  
761 Baker, A. R. and Croot, P. L.: Atmospheric and marine controls on aerosol iron solubility in  
762 seawater, *Mar. Chem.*, doi:10.1016/j.marchem.2008.09.003, 2010.

763  
764 Balseiro, E., Souza, M. S., Serra Olabuenaga, I., Wolinski, L., Bastidas Navarro, M.,  
765 Laspoumaderes, C., & Modenutti, B. (2014). Effect of the Puyehue-Cordon Caulle volcanic  
766 complex eruption on crustacean zooplankton of Andean lakes. *Ecología austral*, 24(1), 75-82.

767

768 Barone, B., Letelier, R. M., Rubin, K. H., & Karl, D. M. (2022). Satellite detection of a massive  
769 phytoplankton bloom following the 2022 submarine eruption of the Hunga Tonga–Hunga  
770 Ha‘apai volcano. *Geophysical Research Letters*, e2022GL099293.  
771  
772 Basedow, Sünnje L., David McKee, Ina Lefering, Astthor Gislason, Malin Daase, Emilia  
773 Trudnowska, Einar Skarstad Egeland, Marvin Choquet, and Stig Falk-Petersen. “Remote Sensing  
774 of Zooplankton Swarms.” *Scientific Reports* 9, no. 1 (2019): 1–10.  
775 <https://doi.org/10.1038/s41598-018-37129-x>.  
776  
777 Behrenfeld, M. J., Boss, E., Siegel, D. A., & Shea, D. M. (2005). Carbon-based ocean  
778 productivity and phytoplankton physiology from space. *Global biogeochemical cycles*, 19(1).  
779  
780 Behrenfeld, M. J., Gaube, P., Della Penna, A., O’malley, R. T., Burt, W. J., Hu, Y., ... & Doney,  
781 S. C. (2019). Global satellite-observed daily vertical migrations of ocean animals. *Nature*,  
782 576(7786), 257-261.  
783  
784 Behrenfeld, M. J., Bisson, K. M., Boss, E., Gaube, P., & Karp-Boss, L. (2022). Phytoplankton  
785 community structuring in the absence of resource-based competitive exclusion. *Plos one*, 17(9),  
786 e0274183.  
787  
788 Bisson, K., Siegel, D. A., & DeVries, T. (2020a). Diagnosing mechanisms of ocean carbon  
789 export in a satellite-based food web model. *Frontiers in Marine Science*, 7, 505.  
790  
791 Bisson, K. M., Baetge, N., Kramer, S. J., Catlett, D., Girling, G., McNair, H., ... & Valentine, D.  
792 L. (2020b). California wildfire burns boundaries between science and art. *Oceanography*, 33(1),  
793 16-19.  
794  
795 Bisson, K. M., Boss, E., Werdell, P. J., Ibrahim, A., Frouin, R., & Behrenfeld, M. J. (2021).  
796 Seasonal bias in global ocean color observations. *Applied optics*, 60(23), 6978-6988.  
797  
798 Boehlert, G. W., & Morgan, J. B. (1985). Turbidity enhances feeding abilities of larval Pacific  
799 herring, *Clupea harengus pallasi*. *Hydrobiologia*, 123(2), 161-170.  
800  
801 Brown, S. K., Loughlin, S. C., Sparks, R. S. J., Vye-Brown, C., Barclay, J., Calder, E., et al.  
802 (2015). Global volcanic hazard and risk, chapter 2 in Loughlin, S. C., Sparks, R. S. J., Brown, S.  
803 K., Jenkins, S. F., and Vye-Brown, C. (eds.), *Global Volcanic Hazards and Risk*, Cambridge:  
804 Cambridge University Press, pp. 81-172. <https://doi.org/10.1017/CBO9781316276273.004>  
805  
806 Browning, T. J., Bouman, H. A., Henderson, G. M., Mather, T. A., Pyle, D. M., Schlosser, C., ...  
807 & Moore, C. M. (2014). Strong responses of Southern Ocean phytoplankton communities to  
808 volcanic ash. *Geophysical Research Letters*, 41(8), 2851-2857.  
809  
810 Browning, T. J., Stone, K., Bouman, H. A., Mather, T. A., Pyle, D. M., Moore, C. M., &  
811 Martinez-Vicente, V. (2015). Volcanic ash supply to the surface ocean—remote sensing of  
812 biological responses and their wider biogeochemical significance. *Frontiers in Marine Science*,  
813 2, 14.

814  
815 Bruckert, J., Hoshyaripour, G. A., Horváth, Á., Muser, L. O., Prata, F. J., Hoose, C., and  
816 Vogel, B.: Online treatment of eruption dynamics improves the volcanic ash and SO<sub>2</sub>  
817 dispersion forecast: case of the 2019 Raikoke eruption, *Atmos. Chem. Phys.*, 22, 3535–  
818 3552, <https://doi.org/10.5194/acp-22-3535-2022>, 2022.

819  
820 Bullard, J. E., M. Baddock, T. Bradwell, et al. 2016. "High Latitude Dust in the Earth System."  
821 *Review of Geophysics* 54 [10.1002/2016RG000518].

822  
823 Camargo, J. A. (2003). Fluoride toxicity to aquatic organisms: a review. *Chemosphere*, 50(3),  
824 251-264.

825  
826 Capaccioni, B. and Mangani, F.: Monitoring of active but quiescent volcanoes using light  
827 hydrocarbon distribution in volcanic gases: the results of 4 years of discontinuous monitoring in  
828 the Campi Flegrei (Italy), *Earth Planet. Sci. Lett.*, 188, 543–555, 2001.

829  
830 Carn, S.A., and N. Krotkov, 2016, Ultraviolet satellite measurements of volcanic ash, in  
*Volcanic Ash* (Elsevier, 2016), pp. 217–231.

831  
832 Carr, J. L., Horváth, Á., Wu, D. L., & Friberg, M. D. (2022). Stereo Plume Height and Motion  
833 Retrievals for the Record-Setting Hunga Tonga-Hunga Ha'apai Eruption of 15 January  
834 2022. *Geophysical Research Letters*, 49(9), e2022GL098131.

835  
836 Cashman, K. V., & Rust, A. C. (2020). Far-travelled ash in past and future eruptions: combining  
837 tephrochronology with volcanic studies. *Journal of Quaternary Science*, 35(1-2), 11-22.

838  
839 Censi, P., L.A. Randazzo, P. Zuddas, F. Saiano, P. Aricò, S. Andò, (2010) Trace element  
840 behaviour in seawater during Etna's pyroclastic activity in 2001: Concurrent effects of nutrients  
841 and formation of alteration minerals, *Journal of Volcanology and Geothermal Research*,  
842 193:106-116, <https://doi.org/10.1016/j.jvolgeores.2010.03.010>.

843  
844 Chase, A. P., Boss, E. S., Haëntjens, N., Culhane, E., Roesler, C., & Karp-Boss, L. (2022).  
845 Plankton Imagery Data Inform Satellite-Based Estimates of Diatom Carbon. *Geophysical  
846 Research Letters*, 49(13), e2022GL098076. <https://doi.org/10.1029/2022GL098076>

847  
848 Chai, T., Crawford, A., Stunder, B., Pavolonis, M. J., Draxler, R., and Stein, A.: Improving volcanic ash  
849 predictions with the HYSPLIT dispersion model by assimilating MODIS satellite retrievals, *Atmos. Chem.  
850 Phys.*, 17, 2865–2879, <https://doi.org/10.5194/acp-17-2865-2017>, 2017.

851  
852 Clarisse, L., Prata, F., Lacour, J.L., Hurtmans, D., Clerbaux, C., Coheur, P.F., 2010a. A  
853 correlation method for volcanic ash detection using hyperspectral infrared measurements.  
854 *Geophys. Res. Lett.*, 37, L19806, <https://doi.org/10.1029/2010GL044828>.

855  
856 Cohen, Jonathan H., and Richard B. Forward Jr. "Zooplankton diel vertical migration—a review  
857 of proximate control." *Oceanography and marine biology* (2016): 89-122.

858  
859 Collister, B. L., Richard C. Zimmerman, V. J. Hill, C. I. Sukenik, and W. M. Balch. "Polarized  
860 Lidar and Ocean Particles: Insights from a Mesoscale Coccolithophore Bloom." *Appl. Opt.* 59,  
861 no. 15 (2020): 4650–62. <https://doi.org/10.1364/AO.389845>.

857  
858 Collister, B. L., Richard C. Zimmerman, C. I. Sukenik, V. J. Hill, and W. M. Balch. “Remote  
859 Sensing of Optical Characteristics and Particle Distributions of the Upper Ocean Using  
860 Shipboard Lidar.” *Remote Sens. Environ.* 115 (2018): 85–96.  
861  
862 Colombier, M., Mueller, S.B., Kueppers, U. et al. Diversity of soluble salt concentrations on  
863 volcanic ash aggregates from a variety of eruption types and deposits. *Bull Volcanol* 81, 39  
864 (2019). <https://doi.org/10.1007/s00445-019-1302-0>  
865  
866 Cornwell, G. C., Sultana, C. M., Prank, M., Cochran, R. E., Hill, T. C. J., Schill, G. P., et al.  
867 (2020). Ejection of dust from the ocean as a potential source of marine ice nucleating particles.  
868 *Journal of Geophysical Research: Atmospheres*, 125, e2020JD033073.  
869 <https://doi.org/10.1029/2020JD033073>  
870  
871 Crawford, A., Chai, T., Wang, B., Ring, A., Stunder, B., Loughner, C. P., Pavolonis, M., and  
872 Sieglaff, J.: Evaluation and bias correction of probabilistic volcanic ash forecasts, *Atmos.*  
873 *Chem. Phys.*, 22, 13967–13996, <https://doi.org/10.5194/acp-22-13967-2022>, 2022.  
874  
875 de Leeuw, J., Schmidt, A., Witham, C. S., Theys, N., Taylor, I. A., Grainger, R. G., Pope, R.  
876 J., Haywood, J., Osborne, M., and Kristiansen, N. I.: The 2019 Raikoke volcanic eruption –  
877 Part 1: Dispersion model simulations and satellite retrievals of volcanic sulfur dioxide,  
878 *Atmos. Chem. Phys.*, 21, 10851–10879, <https://doi.org/10.5194/acp-21-10851-2021>, 2021.  
879  
880 Deguine, A., Petitprez, D., Clarisse, L., Deschutter, L., Fontijn, K., & Herbin, H. (2023).  
881 Retrieval of refractive indices of ten volcanic ash samples in the infrared, visible and ultraviolet  
882 spectral region. *Journal of Aerosol Science*, 167, 106100.  
883  
884 Delmelle, P., Stix, J., Bourque, C. P. A., Baxter, P. J., Garcia-Alvarez, J., & Barquero, J. (2001).  
885 Dry deposition and heavy acid loading in the vicinity of Masaya Volcano, a major sulfur and  
886 chlorine source in Nicaragua. *Environmental science & technology*, 35(7), 1289-1293.  
887  
888 Drazen, J. C., Smith, C. R., Gjerde, K. M., Haddock, S. H., Carter, G. S., Choy, C. A., ... &  
889 Yamamoto, H. (2020). Opinion: Midwater ecosystems must be considered when evaluating  
890 environmental risks of deep-sea mining. *Proceedings of the National Academy of Sciences*,  
891 117(30), 17455-17460.  
892  
893 Duggen S, Olgun N, Croot P, Hoffmann L, Dietze H, et al. 2010. The role of airborne volcanic  
894 ash for the surface ocean biogeochemical iron-cycle: a review. *Biogeosciences* 7:827–44.  
895 <https://doi.org/10.5194/bg-7-827-2010>  
896  
897 Duggen, S., Croot, P., Schacht, U., & Hoffmann, L. (2007). Subduction zone volcanic ash can  
898 fertilize the surface ocean and stimulate phytoplankton growth: Evidence from biogeochemical  
899 experiments and satellite data. *Geophysical research letters*, 34(1).  
900  
901 Echeveste, P., Agustí, S., & Tovar-Sánchez, A. (2012). Toxic thresholds of cadmium and lead to  
902 oceanic phytoplankton: cell size and ocean basin-dependent effects. *Environmental Toxicology*  
903 *and Chemistry*, 31(8), 1887-1894.

904  
905 Eswaran, H., Van Den Berg, E. & Reich, P. 1993. Organic carbon in soils of the world. Soil  
906 Science Society of America Journal, 57, 192–194.  
907  
908 Feng, L., & Hu, C. (2016). Cloud adjacency effects on top-of-atmosphere radiance and ocean  
909 color data products: A statistical assessment. *Remote Sensing of Environment*, 174, 301-313.  
910  
911 Flower, Verity J. B., and Ralph A. Kahn. “Assessing the Altitude and Dispersion of Volcanic  
912 Plumes Using MISR Multi-Angle Imaging from Space: Sixteen Years of Volcanic Activity in  
913 the Kamchatka Peninsula, Russia.” *Journal of Volcanology and Geothermal Research* 337 (May  
914 1, 2017): 1–15. <https://doi.org/10.1016/j.jvolgeores.2017.03.010>.  
915  
916 Flueck, W. T. (2016). The impact of recent volcanic ash depositions on herbivores in Patagonia:  
917 a review. *The Rangeland Journal*, 38(1), 27-34.  
918  
919 Frogner, P., Gislason, S. R., and Oskarsson, N.: Fertilizing potential of volcanic ash in ocean  
920 surface water, *Geology*, 29, 487–490, 2001.  
921  
922 Genareau, K., S. J. Cronin, C. Stewart, S. Bhattacharyya, and R. Donahoe (2016), Posteruptive  
923 impacts of pyroclastic deposits from basaltic andesite stratovolcanoes on surface water  
924 composition, *J. Geophys. Res. Biogeosci.*, 121, 1275–1287, doi:10.1002/2015JG003316.  
925  
926 Gangale, G., Prata, A., Clarisse, L., 2010. The infrared spectral signature of volcanic ash  
927 determined from high-spectral resolution satellite measurements. *Remote Sens. Environ.* 114,  
928 414–425. <https://doi.org/10.1016/j.rse.2009.09.007>.  
929  
930 Go, S., Lyapustin, A., Schuster, G. L., Choi, M., Ginoux, P., Chin, M., Kalashnikova, O.,  
931 Dubovik, O., Kim, J., da Silva, A., Holben, B., and Reid, J. S., 2022. Inferring iron-oxide species  
932 content in atmospheric mineral dust from DSCOVR EPIC observations, *Atmos. Chem. Phys.*,  
933 22, 1395–1423, <https://doi.org/10.5194/acp-22-1395-2022>.  
934  
935 Gordon, H. R., and M. Wang. 1994. Retrieval of water-leaving radiance and aerosol optical  
936 thickness over the oceans with SeaWiFS: a preliminary algorithm. *Appl. Opt.*  
937 doi:10.1364/ao.33.000443.  
938  
939 Gouhier, M., Pinel, V., Belart, J.M.C. et al. CNES-ESA satellite contribution to the  
940 operational monitoring of volcanic activity: The 2021 Icelandic eruption of Mt. Fagradalsfjall.  
941 *J Appl. Volcanol.* 11, 10 (2022). <https://doi.org/10.1186/s13617-022-00120-3>  
942  
943 Gupta, P., R. C. Levy, S. Mattoo, et al. 2019. "Retrieval of aerosols over Asia from the Advanced  
944 Himawari Imager: Expansion of temporal coverage of the global Dark Target aerosol product."  
945 *Atmospheric Measurement Techniques* 12 6557–6577 [10.5194/amt-12-6557-2019]  
946  
947 Haeckel M., van Beusekom J., Wiesner M. G. and Ko'nig I. (2001) The impact of the 1991  
948 Mount Pinatubo tephra fallout on the geochemical environment of the deep-sea sediments in the

949 South China Sea. *Earth Planet. Sci. Lett.* 193, 151–166.

950

951 Hamme, R. C., Webley, P. W., Crawford, W. R., Whitney, F. A., DeGrandpre, M. D., Emerson,

952 S. R., ... & Lockwood, D. (2010). Volcanic ash fuels anomalous plankton bloom in subarctic

953 northeast Pacific. *Geophysical Research Letters*, 37(19).

954

955 Hansen, Agnethe N., and André W. Visser. "Carbon export by vertically migrating zooplankton:

956 an optimal behavior model." *Limnology and Oceanography* 61.2 (2016): 701-710.

957

958 Hecky, R. E., & Kilham, P. (1988). Nutrient limitation of phytoplankton in freshwater and

959 marine environments: a review of recent evidence on the effects of enrichment 1. *Limnology and*

960 *oceanography*, 33(4part2), 796-822.

961

962 Hedley, J. D., Roelfsema, C. M., Chollett, I., Harborne, A. R., Heron, S. F., J. Weeks, S., ... &

963 Mumby, P. J. (2016). Remote sensing of coral reefs for monitoring and management: a

964 review. *Remote Sensing*, 8(2), 118.

965

966 Heiken, G. (1974). Atlas of volcanic ash. *Smithsonian Contributions to the Earth Sciences*.

967

968 Hembury, D.J., M.R. Palmer, G.R. Fones, R.A. Mills, R. Marsh, M.T. Jones, (2012) Uptake of

969 dissolved oxygen during marine diagenesis of fresh volcanic material, *Geochimica et*

970 *Cosmochimica Acta*, 84:353-368, <https://doi.org/10.1016/j.gca.2012.01.017>.

971

972 Henson, S. A., Painter, S. C., Penny Holliday, N., Stinchcombe, M. C., & Giering, S. L. (2013).

973 Unusual subpolar North Atlantic phytoplankton bloom in 2010: volcanic fertilization or North

974 Atlantic Oscillation?. *Journal of Geophysical Research: Oceans*, 118(10), 4771-4780.

975

976 Hoffmann, L. J., Breitbarth, E., Ardelan, M., Duggen, S., Olgun, N., Hassellöv, M., &

977 Wängberg, S.-Å. (2012). Influence of trace metal release from volcanic ash on growth of

978 *Thalassiosira pseudonana* and *Emiliana huxleyi*. *Marine Chemistry*, 132, 28-33.

979

980 Holasek, R. E., and Self, S. (1995), GOES weather satellite observations and measurements of

981 the May 18, 1980, Mount St. Helens eruption, *J. Geophys. Res.*, 100( B5), 8469– 8487,

982 [doi:10.1029/94JB03137](https://doi.org/10.1029/94JB03137).

983 Jones, M. T., & Gislason, S. R. (2008). Rapid releases of metal salts and nutrients following the

984 deposition of volcanic ash into aqueous environments. *Geochimica et Cosmochimica*

985 *Acta*, 72(15), 3661-3680.

986

987 Kawaratani, R. K., & Fujita, S. I. (1990). Wet deposition of volcanic gases and ash in the vicinity

988 of Mount Sakurajima. *Atmospheric Environment. Part A. General Topics*, 24(6), 1487-1492.

989

990 Kockum, P. C. F., Herbert, R. B., & Gislason, S. R. (2006). A diverse ecosystem response to

991 volcanic aerosols. *Chemical Geology*, 231(1-2), 57-66.

992

993 Koffman, B. G., Yoder, M. F., Methven, T., Hanschka, L., Sears, H. B., Saylor, P. L., &

994 Wallace, K. L. (2021). Glacial Dust Surpasses Both Volcanic Ash and Desert Dust in Its Iron

995 Fertilization Potential. *Global Biogeochemical Cycles*, 35(4), e2020GB006821.  
996 <https://doi.org/https://doi.org/10.1029/2020GB006821>  
997

998 Kondragunta, S., Laszlo, I., Zhang, H., Ciren, P., and Huff, A.: Air Quality Applications of ABI  
999 Aerosol Products from the GOES-R Series, in: *The GOES-R Series: A New Generation of*  
1000 *Geostationary Environmental Satellites*, Elsevier, Amsterdam, the Netherlands, Oxford, UK,  
1001 Cambridge MA, USA, 203–217, 2020.  
1002

1003 Krotkov, N. A., Flittner, D. E., Krueger, A. J., Kostinski, A., Riley, C., Rose, W., & Torres, O.  
1004 (1999a). Effect of particle non-sphericity on satellite monitoring of drifting volcanic ash  
1005 clouds. *Journal of Quantitative Spectroscopy and Radiative Transfer*, 63(2-6), 613-630.  
1006

1007 Krotkov, N. A., Torres, O., Seftor, C., Krueger, A. J., Kostinski, A., Rose, W. I., ... & Schaefer,  
1008 S. J. (1999b). Comparison of TOMS and AVHRR volcanic ash retrievals from the August 1992  
1009 eruption of Mt. Spurr. *Geophysical research letters*, 26(4), 455-458.  
1010

1011 Kramer, S. J., Bisson, K. M., & Fischer, A. D. (2020). Observations of phytoplankton  
1012 community composition in the Santa Barbara Channel during the Thomas Fire. *Journal of*  
1013 *Geophysical Research: Oceans*, 125(12), e2020JC016851.  
1014

1015 Kramer, S. J., Siegel, D. A., Maritorea, S., & Catlett, D. (2022). Modeling surface ocean  
1016 phytoplankton pigments from hyperspectral remote sensing reflectance on global scales. *Remote*  
1017 *Sensing of Environment*, 270, 112879. <https://doi.org/10.1016/j.rse.2021.112879>  
1018

1019 Kramer, S. J., Mitchell, C., & Bisson, K. M. (2023). Wildfires change ocean color: a case study  
1020 during the Thomas Fire. *Authorea Preprints*.  
1021

1022 Langmann, B., Zakšek, K., Hort, M., & Duggen, S. (2010). Volcanic ash as fertiliser for the  
1023 surface ocean. *Atmospheric Chemistry and Physics*, 10(8), 3891-3899.  
1024

1025 Langmann, B.: On the role of climate forcing by volcanic sulphate and volcanic ash,  
1026 2014, <https://doi.org/10.1155/2014/340123>, 2014.  
1027

1028 Langmann, B.: Volcanic Ash versus Mineral Dust: Atmospheric Processing and  
1029 Environmental and Climate Impacts, Article ID, 1–17,  
1030 <https://doi.org/10.1155/2013/245076>, 2013.  
1031

1032 Lee, CT.A., Jiang, H., Ronay, E. et al. Volcanic ash as a driver of enhanced organic carbon  
1033 burial in the Cretaceous. *Sci Rep* 8, 4197 (2018). <https://doi.org/10.1038/s41598-018-22576-3>  
1034

1035 Lin, I. I., Hu, C., Li, Y. H., Ho, T. Y., Fischer, T. P., Wong, G. T., ... & Chen, J. P. (2011).  
1036 Fertilization potential of volcanic dust in the low-nutrient low-chlorophyll western North Pacific  
1037 subtropical gyre: Satellite evidence and laboratory study. *Global Biogeochemical Cycles*, 25(1).  
1038

1039 Longman, J., Palmer, M. R., Gernon, T. M., & Manners, H. R. (2019). The role of tephra in  
1040 enhancing organic carbon preservation in marine sediments. *Earth-Science Reviews*, 192, 480–  
1041 490. <https://doi.org/10.1016/j.earscirev.2019.03.018>  
1042

1043 Longman, J., Gernon, T. M., Palmer, M. R., & Manners, H. R. (2021). Tephra deposition and  
1044 bonding with reactive oxides enhances burial of organic carbon in the Bering Sea. *Global  
1045 Biogeochemical Cycles*, 35, e2021GB007140. <https://doi.org/10.1029/2021GB007140>  
1046

1047 Lopez, J. S., Lee, L., & Mackey, K. R. (2019). The toxicity of copper to *Crocospaera watsonii*  
1048 and other marine phytoplankton: a systematic review. *Frontiers in Marine Science*, 5, 511.  
1049

1050 Magruder, L. A., Brunt, K. M., & Alonzo, M. (2020). Early ICESat-2 on-orbit geolocation  
1051 validation using ground-based corner cube retro-reflectors. *Remote Sensing*, 12(21), 3653.  
1052

1053 Mahowald, N. M., Scanza, R., Brahney, J., Goodale, C. L., Hess, P. G., Moore, J. K., & Neff, J.  
1054 (2017). Aerosol deposition impacts on land and ocean carbon cycles. *Current Climate Change  
1055 Reports*, 3(1), 16-31.  
1056

1057 Mahowald, N., Ward, D. S., Kloster, S., Flanner, M. G., Heald, C. L., Heavens, N. G.,  
1058 Hess, P. G., Lamarque, J.-F., and Chuang, P. Y.: Aerosol impacts on climate and  
1059 biogeochemistry, 36, <https://doi.org/10.1146/annurev-environ-042009-094507>, 2011a.  
1060

1061 Mahowald, N., Ward, D. S., Kloster, S., Flanner, M. G., Heald, C. L., Heavens, N. G.,  
1062 Hess, P. G., Lamarque, J.-F., and Chuang, P. Y.: Aerosol Impacts on Climate and  
1063 Biogeochemistry, 36, 45–74, <https://doi.org/10.1146/annurev-environ-042009-094507>,  
1064 2011b.  
1065

1066 Mahowald NM, Hamilton DS, Mackey KRM, Moore JK, Baker AR, et al. 2018. Aerosol trace  
1067 metal leaching and impacts on marine microorganisms. *Nat. Commun.* 9:2614.  
1068 <https://doi.org/10.1038/s41467-018-04970-7>  
1069

1070 Mann, E. L., Ahlgren, N., Moffett, J. W., & Chisholm, S. W. (2002). Copper toxicity and  
1071 cyanobacteria ecology in the Sargasso Sea. *Limnology and Oceanography*, 47(4), 976-988.  
1072

1073 Major, J.J. (2020) Mount St. Helens at 40. *Science*. 368:704-705. DOI: 10.1126/science.abb4120  
1074

1075 Marchese, F, A. Falconieri, N. Pergola, abd V. Tramutoli, A retrospective analysis of the  
1076 Shinmoedake (Japan) eruption of 26–27 January 2011 by means of Japanese geostationary  
1077 satellite data, *Journal of Volcanology and Geothermal Research*,  
1078 <https://doi.org/10.1016/j.jvolgeores.2013.10.011>.  
1079

1079 Markus, T., Neumann, T., Martino, A., Abdalati, W., Brunt, K., Csatho, B., ... & Zwally, J.  
1080 (2017). The Ice, Cloud, and land Elevation Satellite-2 (ICESat-2): science requirements, concept,  
1081 and implementation. *Remote sensing of environment*, 190, 260-273.  
1082

1083 McKinnell, S. (2013). Challenges for the Kasatoshi volcano hypothesis as the cause of a large  
1084 return of sockeye salmon (*Oncorhynchus nerka*) to the Fraser River in 2010. *Fisheries*  
1085 *Oceanography*, 22(4), 337-344.  
1086  
1087 Meinander, O., P. Dagsson-Waldhauserova, P. Amosov, et al. 2022. "Newly identified  
1088 climatically and environmentally significant high-latitude dust sources." *Atmospheric Chemistry*  
1089 *and Physics* 22 (17): 11889-11930 [10.5194/acp-22-11889-2022].  
1090  
1091 Mélançon, J., Levasseur, M., Lizotte, M., Delmelle, P., Cullen, J., Hamme, R. C., ... & Robert,  
1092 M. (2014). Early response of the northeast subarctic Pacific plankton assemblage to volcanic ash  
1093 fertilization. *Limnology and oceanography*, 59(1), 55-67.  
1094  
1095 Mittal, T., & Delbridge, B. (2019). Detection of the 2012 Havre submarine eruption plume using  
1096 Argo floats and its implications for ocean dynamics. *Earth and Planetary Science Letters*, 511,  
1097 105-116.  
1098  
1099 Modenutti BE, Balseiro EG, Elser JJ, Bastidas Navarro M, Cuassolo F, Laspoumaderes C, Souza  
1100 MS, Diaz Villanueva V (2013) Effect of volcanic eruption on nutrients, light, and phytoplankton  
1101 in oligotrophic lakes. *Limnol Oceanogr* 58:1165–1175  
1102  
1103 Moffett, J. W., Brand, L. E., Croot, P. L., & Barbeau, K. A. (1997). Cu speciation and  
1104 cyanobacterial distribution in harbors subject to anthropogenic Cu inputs. *Limnology and*  
1105 *Oceanography*, 42(5), 789-799.  
1106  
1107 Mohr, C. H., Korup, O., Ulloa, H., & Iroumé, A. (2017). Pyroclastic eruption boosts organic  
1108 carbon fluxes into Patagonian fjords. *Global Biogeochemical Cycles*, 31, 1626–1638.  
1109 <https://doi.org/10.1002/2017GB005647>  
1110  
1111 Muser, L. O., Hoshyaripour, G. A., Bruckert, J., Horváth, Á., Malinina, E., Wallis, S., Prata,  
1112 F. J., Rozanov, A., von Savigny, C., Vogel, H., and Vogel, B.: Particle aging and aerosol–  
1113 radiation interaction affect volcanic plume dispersion: evidence from the Raikoke 2019  
1114 eruption, *Atmos. Chem. Phys.*, 20, 15015–15036, <https://doi.org/10.5194/acp-20-15015-2020>,  
1115 2020  
1116  
1117 Newcomb, T. W., & Flagg, T. A. (1983). Volcanic Ash on Juvenile Salmon Smolts. *Marine*  
1118 *Fisheries Review*, 45.  
1119  
1120 Nobileau, D., and D. Antoine. 2005. Detection of blue-absorbing aerosols using near infrared  
1121 and visible (ocean color) remote sensing observations. *Remote Sens. Environ.*  
1122 [doi:10.1016/j.rse.2004.12.020](https://doi.org/10.1016/j.rse.2004.12.020)  
1123  
1124 Ohman, Mark D., and Jean-Baptiste Romagnan. "Nonlinear effects of body size and optical  
1125 attenuation on diel vertical migration by zooplankton." *Limnology and Oceanography* 61.2  
1126 (2016): 765-770.  
1127

1128 Olgun, N., Duggen, S., Croot, P. L., Delmelle, P., Dietze, H., Schacht, U., Óskarsson, N.,  
1129 Siebe, C., Auer, A., Garbe-Schönberg, D., Oskarsson, N., Siebe, C., Auer, A., and Garbe-  
1130 Schonberg, D.: Surface ocean iron fertilization: the role of airborne volcanic ash from  
1131 subduction zone and hot spot volcanoes and related iron fluxes into the Pacific Ocean, 25,  
1132 doi:10.1029/2009GB003761, <https://doi.org/10.1029/2009GB003761>, 2011.  
1133

1134 Olgun N, Duggen S, Andronico D, Kutterolf S, Croot PL, et al. 2013. Possible impacts of  
1135 volcanic ash emissions of Mount Etna on the primary productivity in the oligotrophic  
1136 Mediterranean Sea: results from nutrient-release experiments in seawater. *Mar. Chem.* 152:32–  
1137 42. <https://doi.org/10.1016/j.marchem.2013.04.004>  
1138

1139 Osman, S., Beckett, F., Rust, A., and Snee, E.: Sensitivity of volcanic ash dispersion  
1140 modelling to input grain size distribution based on hydromagmatic and magmatic  
1141 deposits, *Atmosphere (Basel)*, 11, <https://doi.org/10.3390/atmos11060567>, 2020.  
1142

1143 Pangle, Kevin L., et al. "Context-dependent planktivory: interacting effects of turbidity and  
1144 predation risk on adaptive foraging." *Ecosphere* 3.12 (2012): 1-18.  
1145

1146 Pardini, F.; Corradini, S.; Costa, A.; Esposti Ongaro, T.; Merucci, L.; Neri, A.; Stelitano, D.;  
1147 de' Michieli Vitturi, M. Ensemble-Based Data Assimilation of Volcanic Ash Clouds from  
1148 Satellite Observations: Application to the 24 December 2018 Mt. Etna Explosive Eruption.  
1149 *Atmosphere* 2020, 11, 359. <https://doi.org/10.3390/atmos11040359>  
1150

1151 Parsons, T. R., & Whitney, F. A. (2012). Did volcanic ash from Mt. Kasatoshi in 2008 contribute  
1152 to a phenomenal increase in Fraser River sockeye salmon (*Oncorhynchus nerka*) in  
1153 2010?. *Fisheries Oceanography*, 21(5), 374-377.  
1154

1155 Parsons, T., & Whitney, F. (2014). On the effect of the Kasatoshi volcano on the large return of  
1156 sockeye salmon (*Oncorhynchus nerka*) to the Fraser River in 2010. *Fisheries*  
1157 *Oceanography*, 23(1), 101-102.  
1158

1159 Passarelli, L., & Brodsky, E. E. (2012). The correlation between run-up and repose times of  
1160 volcanic eruptions. *Geophysical Journal International*, 188(3), 1025-1045.  
1161

1162 Pavolonis, M. J., J. Sieglaff, & J. Cintineo (2015), Spectrally Enhanced Cloud Objects—A  
1163 generalized framework for automated detection of volcanic ash and dust clouds using passive  
1164 satellite measurements: 1. Multispectral analysis, *J. Geophys. Res. Atmos.*, 120, 7813–7841,  
1165 doi:10.1002/2014JD022968.  
1166

1167 Paytan, A., Mackey, K. R. M., Chen, Y., Lima, I. D., Doney, S. C., Mahowald, N., Labiosa, R.,  
1168 & Post, A. F. (2009). Toxicity of atmospheric aerosols on marine phytoplankton. *Proceedings of*  
1169 *the National Academy of Sciences of the United States of America*, 106(12), 4601-4605.  
1170

1171 Petroff, A. and Zhang, L.: Development and validation of a size-resolved particle dry  
1172 deposition scheme for application in aerosol transport models, 3, 753–769,  
1173 <https://doi.org/10.5194/gmd-3-753-2010>, 2010.

1174  
1175 Pierson, T.C. and Major, J.J. (2014) Hydrogeomorphic Effects of Explosive Volcanic Eruptions  
1176 on Drainage Basins, *Annual Review of Earth and Planetary Sciences* 42:1, 469-507  
1177  
1178 Piontek, D., Hornby, A. J., Voigt, C., Bugliaro, L., & Gasteiger, J. (2021). Determination of  
1179 complex refractive indices and optical properties of volcanic ashes in the thermal infrared based  
1180 on generic petrological compositions. *Journal of Volcanology and Geothermal Research*, 411,  
1181 107174.  
1182  
1183 Platnick, S., King, M. D., Ackerman, S. A., Menzel, W. P., Baum, B. A., Riédi, J. C., & Frey, R.  
1184 A. (2003). The MODIS cloud products: Algorithms and examples from Terra. *IEEE*  
1185 *Transactions on geoscience and Remote Sensing*, 41(2), 459-473.  
1186  
1187 Poland, Michael P., & Anderson, K. R. (2020). Partly cloudy with a chance of lava flows:  
1188 Forecasting volcanic eruptions in the twenty-first century. *Journal of Geophysical Research:*  
1189 *Solid Earth*, 125, e2018JB016974. <https://doi.org/10.1029/2018JB016974>  
1190  
1191 Poland, M. P., Lopez, T., Wright, R., & Pavolonis, M. J. (2020). Forecasting, detecting, and  
1192 tracking volcanic eruptions from space. *Remote Sensing in Earth Systems Sciences*, 3(1), 55-94.  
1193  
1194 Prata F, Lynch M. 2019. Passive earth observations of volcanic clouds in the atmosphere.  
1195 *Atmosphere* 10, <https://doi.org/10.3390/atmos10040199>  
1196  
1197 Randazzo, L. A., Censi, P., Saiano, F., Zuddas, P., Aric`o, P., and Mazzola, S.: Trace elements  
1198 release from volcanic ash to seawater. Natural concentrations in Central Mediterranean Sea,  
1199 European Geosciences Union Meeting, Vienna, 2009  
1200  
1201 Reed, B. E., Peters, D. M., McPheat, R., & Grainger, R. G. (2018). The complex refractive index  
1202 of volcanic ash aerosol retrieved from spectral mass extinction. *Journal of Geophysical*  
1203 *Research: Atmospheres*, 123(2), 1339-1350.  
1204  
1205 Robison, B. H. (2009). Conservation of deep pelagic biodiversity. *Conservation Biology*, 23(4),  
1206 847-858.  
  
1207 Rogers, N. (2015), The Composition and Origin of Magmas, in *The Encyclopedia of Volcanoes*,  
1208 edited by H. Sigurdsson et al., pp. 93-112, Elsevier, London, [http://dx.doi.org/10.1016/B978-0-](http://dx.doi.org/10.1016/B978-0-12-385938-9.00004-3)  
1209 [12-385938-9.00004-3](http://dx.doi.org/10.1016/B978-0-12-385938-9.00004-3).  
  
1210 Rose WI, Bluth GJS, Schneider DJ, et al. 2001. Observations of volcanic clouds in their first few  
1211 days of atmospheric residence: the 1992 eruptions of Crater Peak, Mount Spurr volcano, Alaska.  
1212 *Journal of Geology* 109: 677–694.  
1213  
1214 Rose, W. I., & Durant, A. J. (2009). Fine ash content of explosive eruptions. *Journal of*  
1215 *Volcanology and Geothermal Research*, 186(1-2), 32-39.  
1216  
1217

1218 Ruggieri, F., Fernandez-Turiel, J., Saavedra, J., Gimeno, D., Polanco, E., Amigo, A., Galindo,  
1219 G., & Caselli, A. (2012). Contribution of volcanic ashes to the regional geochemical balance:  
1220 The 2008 eruption of Chaitén volcano, Southern Chile. *Science of the Total Environment*, 425,  
1221 75-88.  
1222  
1223 Schils T (2012) Episodic Eruptions of Volcanic Ash Trigger a Reversible Cascade of Nuisance  
1224 Species Outbreaks in Pristine Coral Habitats. *PLoS ONE* 7(10): e46639.  
1225 <https://doi.org/10.1371/journal.pone.0046639>  
1226  
1227 Schmidt, A., Carslaw, K. S., Mann, G. W., Rap, A., Pringle, K. J., Spracklen, D. V., ... & Forster,  
1228 P. M. (2012). Importance of tropospheric volcanic aerosol for indirect radiative forcing of  
1229 climate. *Atmospheric Chemistry and Physics*, 12(16), 7321-7339.  
1230  
1231 Shkinev, V. M., Ermolin, M. S., Fedotov, P. S., Borisov, A. P., Karandashev, V. K., and  
1232 Spivakov, B. Y.: A set of analytical methods for the estimation of elemental and grain-  
1233 size composition of volcanic ash, 54, 1252–1260,  
1234 <https://doi.org/10.1134/S0016702916130176>, 2016.  
1235  
1236 Siegel, D. A., Wang, M., Maritorena, S., & Robinson, W. (2000). Atmospheric correction of  
1237 satellite ocean color imagery: the black pixel assumption. *Applied optics*, 39(21), 3582-3591.  
1238  
1239 Siringan, F.P., Racasa, E.D.R., David, C.P.C. et al. Increase in Dissolved Silica of Rivers Due to  
1240 a Volcanic Eruption in an Estuarine Bay (Sorsogon Bay, Philippines). *Estuaries and Coasts* 41,  
1241 2277–2288 (2018). <https://doi.org/10.1007/s12237-018-0428-1>  
1242  
1243 Smith, D. B., Zielinski, R. A., and Rose, W. I.: Leachability of uranium and other elements from  
1244 freshly erupted volcanic ash, *J. Volcanol. Geoth. Res.*, 13, 1–30, 1982.  
1245  
1246 Steinberg, Deborah K., and Michael R. Landry. "Zooplankton and the ocean carbon cycle."  
1247 *Annual review of marine science* 9.1 (2017): 413-444.  
1248  
1249 Steinman, B.A., Daniel B. Nelson, Mark B. Abbott, Nathan D. Stansell, Matthew S.  
1250 Finkenbinder, Bruce P. Finney, (2019) Lake sediment records of Holocene hydroclimate and  
1251 impacts of the Mount Mazama eruption, north-central Washington, USA, *Quaternary Science*  
1252 *Reviews*, 204:17-36, <https://doi.org/10.1016/j.quascirev.2018.09.018>.  
1253  
1254 Stevenson JA, Millington SC, Beckett FM, et al. 2015. Big grains go far: reconciling  
1255 tephrochronology with atmospheric measurements of volcanic ash. *Atmospheric Measurement*  
1256 *Techniques Discussions* 8: 65–120.  
1257  
1258 Stewart, C., David E. Damby, Ines Tomašek, Claire J. Horwell, Geoffrey S. Plumlee, Maria  
1259 Aurora Armienta, Maria Gabriela Ruiz Hinojosa, Moya Appleby, Pierre Delmelle, Shane Cronin,  
1260 Christopher J. Ottley, Clive Oppenheimer, Suzette Morman, (2020) Assessment of leachable  
1261 elements in volcanic ashfall: a review and evaluation of a standardized protocol for ash hazard  
1262 characterization, *Journal of Volcanology and Geothermal Research*, 392:106756,  
1263 <https://doi.org/10.1016/j.jvolgeores.2019.106756>.

1264  
1265 Stohl, A., Prata, A. J., Eckhardt, S., Clarisse, L., Durant, A., Henne, S., Kristiansen, N. I.,  
1266 Minikin, A., Schumann, U., Seibert, P., Stebel, K., Thomas, H. E., Thorsteinsson, T.,  
1267 Tørseth, K., and Weinzierl, B.: Determination of time-and height-resolved volcanic ash  
1268 emissions and their use for quantitative ash dispersion modeling: The 2010  
1269 Eyjafjallajökull eruption, 11, 4333–4351, <https://doi.org/10.5194/acp-11-4333-2011>,  
1270 2011.  
1271  
1272 Sunda, W. G., & Huntsman, S. A. (1998). Processes regulating cellular metal accumulation and  
1273 physiological effects: phytoplankton as model systems. *Science of the Total Environment*,  
1274 219(2-3), 165-181.  
1275  
1276 Tayag, J. C., & Punongbayan, R. S. (1994). Volcanic disaster mitigation in the Philippines:  
1277 experience from Mt. Pinatubo. *Disasters*, 18(1), 1-15.  
1278  
1279 Taylor, H. E. and Lichte, F. E.: Chemical composition of Mount St. Helens volcanic ash,  
1280 *Geophys. Res. Lett.*, 7, 949–952, 1980.  
1281  
1282 Thordarson, T., & Self, S. (2003). Atmospheric and environmental effects of the 1783–1784  
1283 Laki eruption: A review and reassessment. *Journal of Geophysical Research: Atmospheres*,  
1284 108(D1), AAC 7-1-AAC 7-29.  
1285  
1286 Tonneijck, F. H., Jansen, B., Nierop, K. G. J., Verstraten, J. M., Sevink, J., and De Lange, L.  
1287 (2010). Towards Understanding of Carbon Stocks and Stabilization in Volcanic Ash Soils in  
1288 Natural Andean Ecosystems of Northern Ecuador. *Eur. J. Soil Sci.* 61, 392–405.  
1289 doi:10.1111/j.1365-2389.2010.01241.x  
1290  
1291 Umazano, A.M. and Melchor, R.N. (2020) Volcaniclastic sedimentation influenced by logjam  
1292 breakups? An example from the Blanco River, Chile. *Journal of South American Earth Sciences*,  
1293 98:102477, <https://doi.org/10.1016/j.jsames.2019.102477>.  
1294  
1295 Utne-Palm, Anne C. "Visual feeding of fish in a turbid environment: physical and behavioural  
1296 aspects." *Marine and Freshwater Behaviour and Physiology* 35.1-2 (2002): 111-128.  
1297  
1298 Urmy, S. S., Williamson, C. E., Leach, T. H., Schladow, S. G., Overholt, E. P., & Warren, J. D.  
1299 (2016). Vertical redistribution of zooplankton in an oligotrophic lake associated with reduction  
1300 in ultraviolet radiation by wildfire smoke. *Geophysical Research Letters*, 43(8), 3746-3753.  
1301  
1302 Vogel, A., S. Diplas, A. J. Durant, A. S. Azar, M. F. Sunding, W. I. Rose, A. Sytchkova, C.  
1303 Bonadonna, K. Krüger, and A. Stohl (2017), Reference data set of volcanic ash physicochemical  
1304 and optical properties, *J. Geophys. Res. Atmos.*, 122, 9485–9514, doi:10.1002/2016JD026328.  
1305  
1306 Vroom, P. S., & Zgliczynski, B. J. (2011). Effects of volcanic ash deposits on four functional  
1307 groups of a coral reef. *Coral Reefs*, 30(4), 1025-1032.

1308 Weinbauer, M.G., Benjamin Guinot, Christophe Migon, Francesca Malfatti, Xavier Mari (2017)  
1309 Skyfall—neglected roles of volcano ash and black carbon rich aerosols for microbial plankton in  
1310 the ocean, *Journal of Plankton Research*, 39:187–198, <https://doi.org/10.1093/plankt/fbw100>  
1311

1312 Wells, A. F., Jones, A., Osborne, M., Damany-Pearce, L., Partridge, D. G., and Haywood, J.  
1313 M.: Including ash in UKESM1 model simulations of the Raikoke volcanic eruption reveals  
1314 improved agreement with observations, *Atmos. Chem. Phys.*, 23, 3985–  
1315 4007, <https://doi.org/10.5194/acp-23-3985-2023>, 2023.  
1316

1317 Westberry, T. K., Shi, Y. R., Yu, H., Behrenfeld, M. J., & Remer, L. A. (2019). Satellite-  
1318 Detected Ocean Ecosystem Response to Volcanic Eruptions in the Subarctic Northeast Pacific  
1319 Ocean. *Geophysical Research Letters*, 46(20), 11270-11280.  
1320

1321 Werdell, P. J., Behrenfeld, M. J., Bontempi, P. S., Boss, E., Cairns, B., Davis, G. T., ... & Remer,  
1322 L. A. (2019). The Plankton, Aerosol, Cloud, ocean Ecosystem mission: status, science,  
1323 advances. *Bulletin of the American Meteorological Society*, 100(9), 1775-1794.  
1324

1325 Wilson, S. T., Hawco, N. J., Armbrust, E. V., Barone, B., Björkman, K. M., Boysen, A. K., ... &  
1326 Karl, D. M. (2019). Kīlauea lava fuels phytoplankton bloom in the North Pacific Ocean. *Science*,  
1327 365(6457), 1040-1044.  
1328

1329 Witham, C. S., Oppenheimer, C., and Horwell, C. J.: Volcanic ash leachates: a review and  
1330 recommendations for sampling methods, *J. Volcanol. Geoth. Res.*, 141, 299–326, 2005.  
1331

1332 Zimanowski, B., Wohletz, K., Dellino, P., & Büttner, R. (2003). The volcanic ash  
1333 problem. *Journal of Volcanology and Geothermal Research*, 122(1-2), 1-5.  
1334

1335 Zimmermann, M., Ruggerone, G. T., Freymueller, J. T., Kinsman, N., Ward, D. H., & Hogrefe,  
1336 K. R. (2018). Volcanic ash deposition, eelgrass beds, and inshore habitat loss from the 1920s to  
1337 the 1990s at Chignik, Alaska. *Estuarine, Coastal and Shelf Science*, 202, 69-86.